Weierstraß-Institut
für Angewandte Analysis und Stochastik

Leibniz-Institut im Forschungsverbund Berlin e. V.

Preprint ISSN 2198-5855

Guaranteed upper bounds for the velocity error of pressure-robust Stokes discretisations

Philip Lukas Lederer[1], Christian Merdon [2]

submitted: August 17, 2020 (revision: July 6, 2021)

[1] TU Wien
Institute for Analysis and Scientific Computing
Wiedner Hauptstraße 8-10
1040 Wien
Austria
E-Mail: philip.lederer@tuwien.ac.at

[2] Weierstrass Institute
Mohrenstr. 39
10117 Berlin
Germany
E-Mail: christian.merdon@wias-berlin.de

No. 2750
Berlin 2020

2010 *Mathematics Subject Classification.* 65N15, 65N30, 76D07, 76M10.

2008 *Physics and Astronomy Classification Scheme.* 47.10.ad, 47.11.Fg.

Key words and phrases. Incompressible Navier–Stokes equations, mixed finite elements, pressure-robustness, a posteriori error estimators, equilibrated fluxes, adaptive mesh refinement.

Philip L. Lederer has been funded by the Austrian Science Fund (FWF) through the research program “Taming complexity in partial differential systems” (F65) - project “Automated discretization in multiphysics” (P10).

Edited by
Weierstraß-Institut für Angewandte Analysis und Stochastik (WIAS)
Leibniz-Institut im Forschungsverbund Berlin e. V.
Mohrenstraße 39
10117 Berlin
Germany

Fax: +49 30 20372-303
E-Mail: preprint@wias-berlin.de
World Wide Web: http://www.wias-berlin.de/

Guaranteed upper bounds for the velocity error of pressure-robust Stokes discretisations

Philip Lukas Lederer, Christian Merdon

ABSTRACT. This paper aims to improve guaranteed error control for the Stokes problem with a focus on pressure-robustness, i.e. for discretisations that compute a discrete velocity that is independent of the exact pressure. A Prager–Synge type result relates the velocity errors of divergence-free primal and perfectly equilibrated dual mixed methods for the velocity stress. The first main result of the paper is a framework with relaxed constraints on the primal and dual method. This enables to use a recently developed mass conserving mixed stress discretisation for the design of equilibrated fluxes and to obtain pressure-independent guaranteed upper bounds for any pressure-robust (not necessarily divergence-free) primal discretisation. The second main result is a provably efficient local design of the equilibrated fluxes with comparably low numerical costs. Numerical examples verify the theoretical findings and show that efficiency indices of our novel guaranteed upper bounds are close to one.

1. INTRODUCTION

In recent years many pressure-robust discretisations for the Stokes equations were found and propagated that avoid a consistency error that is connected to a relaxation of the divergence constraint [21, 25, 28, 31, 26, 18, 46]. In non-pressure-robust discretisation this consistency error can cause severe discretisation errors in presence of large irrotational forces in the right-hand side forcing or, more importantly, in the material derivative of the full Navier–Stokes equations [14, 1]. Pressure-robustness is achieved by using divergence-free finite element methods like [42, 19, 13], but also many classical non-divergence-free methods can be turned pressure-robust by employing a reconstruction operator on the test functions when pairing them with irrotational forces [21, 31, 26]. As a result, a pressure-robust method allows pressure-independent a priori velocity error estimates.

In terms of a posteriori error control the pressure-robustness property of a scheme also allows, in principle, separate error control of the velocity alone and adaptive mesh refinement that is not polluted by a concentration on the pressure error. However, this requires that the evaluation of the a posteriori error estimator itself is pressure-independent. There is a long history on a posteriori error control for the Stokes problem [44, 7, 2, 8, 45, 20, 37] but none of them can be considered to be fully suitable for the error control of the velocity error of a pressure-robust discretisation of the Stokes problem. Recent refined residual-based approaches in the spirit of [27, 22] enable a pressure-robust error control of the velocity error by applying the curl operator to the residual, following the general idea that the velocity is only determined by the underlying vorticity equation.

In this paper we turn our interest to guaranteed error control for the velocity and thereby refine existing approaches in [20, 37, 6, 30, 35] that can become inefficient when used to estimate the velocity error of pressure-robust discretisations.

For simplicity, consider the Stokes problem in d dimensions

$$\begin{aligned} -\nu\Delta\boldsymbol{u} + \nabla p &= \boldsymbol{f} \quad \text{on } \Omega,\\ \mathrm{div}(\boldsymbol{u}) &= 0 \quad \text{on } \Omega. \end{aligned}$$

with homogeneous Dirichlet boundary data and some right-hand side forcing $\boldsymbol{f}$. Here $\boldsymbol{u}$ and p denote the velocity and pressure, respectively, and ν is the kinematic viscosity. There are situations where $\boldsymbol{f}$ can have a large irrotational forcing, e.g. an approximation to the the material derivative $\boldsymbol{u}_t + (\boldsymbol{u}\cdot\nabla)\boldsymbol{u}$. Hence, looking at the unrescaled Stokes model problem with $\nu \neq 1$ is reasonable and numerical discretisations that are robust with respect to large pressures or small viscosities ν are desirable.

Coming back to a posteriori error control, a unified approach as e.g. in [7, 20] rewrites many second order elliptic problems into the form

$$-\mathrm{div}(\widetilde{\sigma}) = \boldsymbol{f} \quad \text{on } \Omega. \tag{1}$$

which is also possible for the Stokes problem above utilizing the pseudo-stress $\widetilde{\sigma} := \nu\nabla\boldsymbol{u} - pI_{d\times d}$, where $I_{d\times d}$ is the d-dimensional identity matrix. Hence, the application of the classical a posteriori error estimators for

DOI 10.20347/WIAS.PREPRINT.2750 Berlin, August 17, 2020/rev. July 6, 2021

(vector-valued) Poisson problems, in particular guaranteed upper bounds like [11, 33, 5, 12, 39, 15], also work for the Stokes problem. However, this approach in general leads to pressure-dependent velocity error estimators or estimators that are only efficient with respect to the combined velocity and pressure error.

Going one step back there is also the famous Prager–Synge theorem [38, 3] (originally for linear elasticity) that is nothing else than a Pythagoras theorem in L^2-norms, i.e.

$$\|\nabla(\boldsymbol{u}-\bar{\boldsymbol{u}}_h)\|^2_{L^2(\Omega)} + \nu^{-1}\|\sigma-\sigma_h\|^2_{L^2(\Omega)} = \|\nabla\bar{\boldsymbol{u}}_h - \nu^{-1}\sigma_h\|^2_{L^2(\Omega)},$$

where $\bar{\boldsymbol{u}}_h$ and σ_h can be understood as some (not necessarily discrete) approximations to $\boldsymbol{u}$ and its stress $\sigma := \nu\nabla\boldsymbol{u}$. If both approximations are known the quantity on the right-hand side yields an a posteriori error estimator for both errors on the left-hand side. However, $\bar{\boldsymbol{u}}_h$ and σ_h have to satisfy some properties for the equality above to hold. In our Stokes setting it is required that $\boldsymbol{u}, \bar{\boldsymbol{u}}_h \in \boldsymbol{V}_0$ and

$$\int_\Omega (\operatorname{div}(\sigma_h) + \boldsymbol{f})\cdot\boldsymbol{v}\,\mathrm{d}x = 0 \quad \text{for all } \boldsymbol{v}\in\boldsymbol{V}_0 \tag{2}$$

where $\boldsymbol{V}_0$ is the subspace of divergence-free $\boldsymbol{H}^1_0(\Omega)$ functions. In comparison with (1) where the divergence constraint for the fixed pseudo-stress has to hold pointwise for the whole space $\boldsymbol{H}^1_0(\Omega)$, equation (2) is not only satisfied by σ_h but also by $\sigma_h - qI_{d\times d}$ for any $q\in H^1(\Omega)$ due to $\int_\Omega \nabla q\cdot\boldsymbol{v}\,\mathrm{d}x = -\int_\Omega q\operatorname{div}(\boldsymbol{v})\,\mathrm{d}x = 0$ for all $\boldsymbol{v}\in\boldsymbol{V}_0$. Hence, the stress approximation σ_h can be gauged by any gradient force to e.g. mimic the pseudo-stress $\widetilde{\sigma}$.

Consider now some discrete velocity $\bar{\boldsymbol{u}}_h$ and pressure $\bar{p}_h$ from some possibly pressure-robust discretisation of the Stokes equations. Many equilibration error estimators, see e.g. [20] where unfortunately only $\nu=1$ is examined, employ the discrete pseudo-stress and fix the gauging freedom by the discrete pressure $q=\bar{p}_h$, e.g. they compute $\widetilde{\sigma}_h$ with

$$\operatorname{div}(\widetilde{\sigma}_h) + \boldsymbol{\pi}_{k-1}\boldsymbol{f} = \operatorname{div}(\sigma_h + \bar{p}_h I_{d\times d}) + \boldsymbol{\pi}_{k-1}\boldsymbol{f} = 0 \tag{3}$$

where $\boldsymbol{\pi}_{k-1}$ is the L^2 best-approximation into the piecewise polynomials of order $k-1$ and k is related to the expected rate of the primal method. Following e.g. [20], one can compute equilibrated fluxes $\widetilde{\sigma}_h$ with this constraint that are close to the discrete pseudo-stress $\nu\nabla\bar{\boldsymbol{u}}_h + \bar{p}_h I_{d\times d}$ and would get the guaranteed upper bound

$$\|\nabla(\boldsymbol{u}-\bar{\boldsymbol{u}}_h)\|^2_{L^2(\Omega)} \le \nu^{-1}\sum_{T\in\mathcal{T}}\left(\frac{h_T}{\pi}\|(\mathbf{id}-\boldsymbol{\pi}_{k-1})\boldsymbol{f}\|_{L^2(T)} + \|\widetilde{\sigma}_h - \bar{p}_h I_{d\times d} - \nu\nabla\bar{\boldsymbol{u}}_h\|_{L^2(T)}\right)^2 \tag{4}$$

which up to the oscillation term resembles the Prager–Synge calculus for $\sigma_h = \widetilde{\sigma}_h - \bar{p}_h I_{d\times d}$. However, the numerical examples below demonstrate that the dependence of this error estimator on the discrete pressure can cause arbitrarily large efficiency indices $\eta/\|\nabla(\boldsymbol{u}-\bar{\boldsymbol{u}}_h)\|$ in pressure-dominant situations where $\boldsymbol{f}$ has a large irrotational part, which can also affect the quality of the adaptive mesh refinement.

In this paper we propose a novel equilibration design that avoids the pseudo-stress approach altogether and instead ensures the Prager–Synge equilibration condition (2) for an $H(\operatorname{div})$-conforming subspace of $\boldsymbol{V}_0$. This is done with the help of the recently developed mass conserving mixed stress formulation [18]. The resulting error estimator for a divergence-free discretisation, with a comparable approximation order k for the equilibrated fluxes, structurally looks very similar to (4), but consists of the terms

$$\|\nabla(\boldsymbol{u}-\bar{\boldsymbol{u}}_h)\|^2_{L^2(\Omega)} \le \nu^{-1}\sum_{T\in\mathcal{T}}\left(ch_T^2\|(\mathbf{id}-\boldsymbol{\pi}_{k-2})\operatorname{curl}(\boldsymbol{f})\|_{L^2(T)} + \|\operatorname{dev}(\sigma_h - \nu\nabla\bar{\boldsymbol{u}}_h)\|_{L^2(T)}\right)^2,$$

where $\operatorname{dev}(A) := A - \frac{\operatorname{tr}(A)}{d}I_{d\times d}$, is the deviatoric part of a matrix $A\in\mathbb{R}^{d\times d}$, and $\operatorname{tr}(A)$ is its matrix trace. Note that there is no dependency on the pressure or the irrotational part of $\boldsymbol{f}$. The unfortunately unknown constant c stems from approximation properties of commuting interpolators and only depends on the shape of the cells in the triangulation. A more general result also shows guaranteed upper bounds for non-divergence-free but pressure-robust discretisations by accounting for the additional divergence of the discrete velocity. The final main result of the paper concerns a less costly localized pressure-robust design for the equilibrated fluxes based on small problems on node patches, which is shown to be locally efficient.

DOI 10.20347/WIAS.PREPRINT.2750 Berlin, August 17, 2020/rev. July 6, 2021

The rest of the paper is organised as follows. Section 2 introduces the Stokes model problem and a related Prager–Synge-type theorem. Section 3 recalls variants of pressure-robust discretisations of the Stokes problem in the primal formulation. After shortly summarising classical equilibration error estimator approaches in Section 4, Section 5 proves a novel framework for pressure-independent guaranteed upper bounds in the spirit of the Prager–Synge theorem but with relaxed constraints. A global design of suitable equilibrated fluxes for the novel framework based on a recently developed mass-conserving mixed stress formulation is discussed in Section 6. The less costly local design for the equilibrated fluxes is presented in Section 7. Section 8 is concerned with the local efficiency of the local error estimator estimators. Finally, Section 9 shows in several numerical examples that the novel upper bounds are indeed pressure-independent and allow very sharp error control and optimal adaptive mesh refinement for the velocity error of pressure-robust discretisations.

Throughout this work we use bold-face notation for vector-valued functions and spaces, but stick to a standard notation for matrix-valued functions and spaces to increase readability. We denote by $L^2(\Omega)$ the space of square integrable functions and by $H^s(\Omega)$ the standard Sobolev space with regularity s. Of special interest is the H^1 space with homogeneous boundary conditions denoted by $H^1_0(\Omega)$. Restricted L^2-norms on subsets $\omega \subset \Omega$ are denoted by $\|\cdot\|_\omega$, while for $\omega = \Omega$ we simply write $\|\cdot\|$. The L^2-inner product on ω and Ω is written as $(\cdot,\cdot)_\omega$ and $(\cdot,\cdot)$, respectively. For high order Sobolev spaces we use the standard notation, hence $\|\cdot\|_{H^s(\omega)}$ denotes the H^s-norm on ω, and as before, $\|\cdot\|_{H^s} = \|\cdot\|_{H^s(\Omega)}$.

2. The Stokes model problem and a Prager–Synge theorem

This section recalls the continuous Stokes model problem and a characterisation of pressure-robustness. Then, a Prager-Synge theorem for the Stokes problem as a point of departure for a posteriori error control is discussed.

2.1. **The Stokes model problem.** Given $\boldsymbol{f} \in L^2(\Omega)$ on some open, bounded domain $\Omega \subset \mathbb{R}^d$ $(d = 2, 3)$ with polygonal or polyhedral boundary, the Stokes model problem with homogeneous Dirichlet boundary data seeks a velocity $\boldsymbol{u} \in \boldsymbol{V} := \boldsymbol{H}^1_0(\Omega)$ and some pressure $p \in Q := L^2_0(\Omega) = \{q \in L^2(\Omega) : (q, 1) = 0\}$ with

$$\begin{aligned} -\nu\Delta\boldsymbol{u} + \nabla p &= \boldsymbol{f} \quad \text{on } \Omega, \\ \operatorname{div}(\boldsymbol{u}) &= 0 \quad \text{on } \Omega, \end{aligned}$$

where $\nu > 0$ is the kinematic viscosity. The regularity assumptions of $\boldsymbol{u}$ and p above allow to expect a weak solution that satisfies

$$\nu(\nabla\boldsymbol{u}, \nabla\boldsymbol{v}) - (p, \operatorname{div}(\boldsymbol{v})) = (\boldsymbol{f}, \boldsymbol{v}) \quad \text{for all } \boldsymbol{v} \in \boldsymbol{V}, \tag{5}$$

$$(\operatorname{div}(\boldsymbol{u}), q) = 0 \quad \text{for all } q \in Q. \tag{6}$$

Note that the pressure acts as a Lagrange multiplier for the divergence constraint. Within the subspace of divergence-free functions

$$\boldsymbol{V}_0 := \{\boldsymbol{v} \in \boldsymbol{V} : \operatorname{div}(\boldsymbol{v}) = 0\} = \{\boldsymbol{v} \in \boldsymbol{V} : \forall q \in Q,\ (q, \operatorname{div}(\boldsymbol{v})) = 0\}.$$

the weak velocity solution $\boldsymbol{u}$ can also be characterised by requiring $\boldsymbol{u} \in \boldsymbol{V}_0$ and

$$\nu(\nabla\boldsymbol{u}, \nabla\boldsymbol{v}) = (\sigma, \nabla\boldsymbol{v}) = (\boldsymbol{f}, \boldsymbol{v}) \quad \text{for all } \boldsymbol{v} \in \boldsymbol{V}_0,$$

with its exact stress given by $\sigma := \nu\nabla\boldsymbol{u}$.

2.2. **Characterising pressure-robustness.** According to the Helmholtz-Hodge decomposition, see e.g. [16] for a proof, any force $\boldsymbol{f} \in \boldsymbol{L}^2(\Omega)$ can be uniquely decomposed into

$$\boldsymbol{f} = \nabla q + \mathbb{P}\boldsymbol{f},$$

with $q \in H^1(\Omega)/\mathbb{R}$ and the (unique) divergence-free Helmholtz–Hodge projector

$$\mathbb{P}\boldsymbol{f} \in \{\boldsymbol{v} \in \boldsymbol{L}^2(\Omega) : \forall q \in H^1(\Omega), (\boldsymbol{v}, \nabla q) = 0\}.$$

Due to $(\nabla q, \boldsymbol{v}) = -(q, \operatorname{div} \boldsymbol{v}) = 0$ for all $\boldsymbol{v} \in \boldsymbol{V}_0$, the velocity solution $\boldsymbol{u}$ of the Stokes problem is not affected by any gradient force. Indeed, from the above decomposition we see that

$$\nu(\nabla \boldsymbol{u}, \nabla \boldsymbol{v}) = (\mathbb{P}\boldsymbol{f}, \boldsymbol{v}) \quad \text{for all } \boldsymbol{v} \in \boldsymbol{V}_0.$$

A discretisation that computes a velocity that preserves this property, and is independent of any gradient force ∇q that is added to the right-hand side, is called pressure-robust (since the pressure gradient is part of the irrotational part of $\boldsymbol{f}$), see [21, 31] for details.

2.3. **A Prager–Synge-type result for the Stokes system.** This section states a Pythagoras theorem for the Stokes system similar to that of Prager and Synge for the Poisson model problem and the linear elasticity problem [38, 3]. The Prager–Synge theorem relates the error of primal and equilibrated mixed approximations of the flux $\nabla \boldsymbol{u}$ (or $\varepsilon(\boldsymbol{u})$ in elasticity) and gives rise to guaranteed error control by the design of equilibrated fluxes for these problems. The analogue in the context of the Stokes model problem for the flux of the velocity $\sigma = \nu \nabla \boldsymbol{u}$ reads as follows.

Theorem 2.1. Consider the solution $\boldsymbol{u} \in \boldsymbol{V}_0(\Omega)$ of the Stokes equation (5), any function $\boldsymbol{u}^{\text{approx}} \in \boldsymbol{V}_0(\Omega)$ and any $\sigma^{\text{approx}} \in H(\operatorname{div}, \Omega)$ with the equilibration constraint

$$(\boldsymbol{f} + \operatorname{div}(\sigma^{\text{approx}}), \boldsymbol{v}) = 0 \quad \text{for all } \boldsymbol{v} \in \boldsymbol{V}_0. \tag{7}$$

Then, there holds the Pythagoras theorem

$$\|\nabla(\boldsymbol{u} - \boldsymbol{u}^{\text{approx}})\|^2 + \nu^{-1}\|\sigma - \sigma^{\text{approx}}\|^2 = \|\nabla \boldsymbol{u}^{\text{approx}} - \nu^{-1}\sigma^{\text{approx}}\|^2.$$

Proof. This follows directly from integration by parts and

$$\begin{aligned}\|\nabla(\boldsymbol{u} - \boldsymbol{u}^{\text{approx}})\|^2 + \|\nabla \boldsymbol{u} - \nu^{-1}\sigma^{\text{approx}}\|^2 - \|\nabla \boldsymbol{u}^{\text{approx}} - \nu^{-1}\sigma^{\text{approx}}\|^2 \\ = 2(\nabla \boldsymbol{u} - \nu^{-1}\sigma^{\text{approx}}, \nabla(\boldsymbol{u} - \boldsymbol{u}^{\text{approx}})) \\ = 2\nu^{-1}(\boldsymbol{f} + \operatorname{div}(\sigma^{\text{approx}}), \boldsymbol{u} - \boldsymbol{u}^{\text{approx}}) = 0.\end{aligned}$$

The last step follows from $\boldsymbol{v} = \boldsymbol{u} - \boldsymbol{u}^{\text{approx}} \in \boldsymbol{V}_0(\Omega)$ and (7). □

Hence, the evaluation of the quantity on the right-hand side for known approximations σ^{approx} and $\boldsymbol{u}^{\text{approx}}$ yields guaranteed upper bounds for the two unknown errors on the left-hand side of the identity. In this paper we consider $\boldsymbol{u}^{\text{approx}}$ as an approximation from a pressure-robust discretisation of the Stokes equations. Then, the computation of a suitable σ^{approx} is the task of the a posteriori error control.

In practise however, both constraints on the function $\boldsymbol{u}^{\text{approx}}$ and on the flux σ^{approx} in Theorem 2.1 are hard to realise. Therefore, Section 5 derives guaranteed upper bounds for $\boldsymbol{u}^{\text{approx}}$ that do not necessarily have to stem from a divergence-free (but pressure-robust) discretisation based on equilibrated fluxes σ^{approx} that satisfy a suitably discretised version of the equilibration property (7).

Section 4 discusses pseudo-stress related equilibration conditions like $\boldsymbol{f} - \nabla q + \operatorname{div}(\sigma^{\text{approx}}) = 0$ for some known (pressure approximation) q as they are used by classical equilibrated flux designs. However, this may lead to a dependency of $p - q$ in the efficiency estimates of the resulting error estimator and the whole focus of pressure-robust discretisations is on how to avoid this. Therefore Section 5 only replaces the space $\boldsymbol{V}_0$ in (7) by some $H(\operatorname{div}, \Omega)$-conforming subspace.

Before that some suitable pressure-robust finite element methods to compute $\boldsymbol{u}^{\text{approx}}$ are revisited.

3. Pressure-robust finite element methods for the Stokes problem

This section recalls pressure-robust discretisations for the primal velocity-pressure formulation of the Stokes problem.

$\bar{\boldsymbol{V}}_h$	$\bar{Q}_h$	abbreviation	r	$\mathcal{R}$
$\boldsymbol{P}_2(\mathcal{T}) \cap \boldsymbol{H}^1_0(\Omega)$	$P_0(\mathcal{T})$	P20	1	I_{BDM_1}
$\boldsymbol{P}_3(\mathcal{T}) \cap \boldsymbol{H}^1_0(\Omega)$	$P_1(\mathcal{T})$	P31	2	I_{BDM_2}
$\boldsymbol{P}_{2+}(\mathcal{T}) \cap \boldsymbol{H}^1_0(\Omega)$	$P_1(\mathcal{T})$	P2B	2	I_{BDM_2}
$\boldsymbol{P}^{\mathrm{3d}}_{2,+}(\mathcal{T}) \cap \boldsymbol{H}^1_0(\Omega)$	$P_1(\mathcal{T})$	P2B-3d	2	I_{BDM_2}
$\boldsymbol{P}_2(\mathcal{T}) \cap \boldsymbol{H}^1_0(\Omega)$	$P_1(\mathcal{T})$	SV	2	$\mathbf{id}$

TABLE 1. Considered inf-sup stable Stokes pairs including the expected order of convergence and the used reconstruction operator.

3.1. **Notation.** Consider some triangulation $\mathcal{T}$ of the domain Ω into regular simplices with vertices $\mathcal{V}$ and faces $\mathcal{F}$. The subset of interior faces is denoted by $\mathcal{F}(\Omega)$. The diameter of a simplex $T \in \mathcal{T}$ is given by h_T. We extend this notation in a similar manner onto faces and simply write h_F for the diameter of a face $F \in \mathcal{F}$. Further, if the triangulation is quasi uniform, we abbreviate the notation and simply write h for the maximum diameter of all simplices.

In the following let $F \in \mathcal{F}$ be some arbitrary face of an arbitrary element $T \in \mathcal{T}$, i.e. $F \subset \partial T$. On F we then denote by $\boldsymbol{n}$ the outward pointing unit normal with respect to T, and

$$\boldsymbol{a}_n := \boldsymbol{a} \cdot \boldsymbol{n}, \quad \text{and} \quad \boldsymbol{a}_t := \boldsymbol{a} - (\boldsymbol{a} \cdot \boldsymbol{n})\boldsymbol{n},$$

denote the scalar-valued normal and the vector-valued tangential trace of some vector $\boldsymbol{a} \in \mathbb{R}^d$, respectively. Further the brackets $[\![b]\!]$ denote the jump on a common face F of two adjacent elements of some (scalar or vector-valued) quantity b.

The space of element-wise (with respect to $\mathcal{T}$) polynomials of order k is denoted by $P_k(\mathcal{T})$ and the space of piece-wise vector-valued polynomials of order k by $\boldsymbol{P}_k(\mathcal{T})$. The L^2 best-approximation into $P_k(\mathcal{T})$ or $\boldsymbol{P}_k(\mathcal{T})$ reads as π_k or $\boldsymbol{\pi}_k$, respectively.

The spaces

$$\begin{aligned}\mathrm{RT}_k(\mathcal{T}) &:= \{\boldsymbol{v}_h \in H(\mathrm{div},\Omega) : \forall T \in \mathcal{T}\, \exists \boldsymbol{a}_T \in \boldsymbol{P}_k(T), b_T \in P_k(T),\, \boldsymbol{v}_h|_T(\boldsymbol{x}) = \boldsymbol{a}_T + b_T\boldsymbol{x}\},\\ \mathrm{BDM}_k(\mathcal{T}) &:= H(\mathrm{div},\Omega) \cap \boldsymbol{P}_k(\mathcal{T})\end{aligned}$$

read as the Raviart–Thomas and Brezzi–Douglas–Marini functions of order $k \geq 0$. Moreover,

$$\mathcal{N}_k(\mathcal{T}) := \{\boldsymbol{v}_h \in H(\mathrm{curl},\Omega) : \forall T \in \mathcal{T}\, \exists \boldsymbol{a}_T \in \boldsymbol{P}_k(T), B_T \in P_k(T)^{d\times d,\mathrm{skw}}, \boldsymbol{v}_h|_T(\boldsymbol{x}) = \boldsymbol{a}_T + B_T\boldsymbol{x}\}$$

denote the space of Nédélec functions of order $k \geq 0$, where $P_k(T)^{d\times d,\mathrm{skw}}$ denotes the space of skew symmetric matrix-valued polynomials of order k. Note that the space $\mathcal{N}_k(\mathcal{T})$ is in the literature, see for example [36], sometimes also called the Nédélec space of order $k+1$ (and not k as in this work). However, we used this notation so that it matches with the definition of the Raviart–Thomas space. For the analysis we denote by $H^s(\mathcal{T})$ the broken Sobolev space of order s with respect to the triangulation $\mathcal{T}$, i.e.

$$H^s(\mathcal{T}) := \{v \in L^2(\Omega), \forall T \in \mathcal{T}, v|_T \in H^s(T)\},$$

with the corresponding norm $\|\cdot\|_{H^s(\mathcal{T})}$, and extend this notation also to vector-valued versions.

Finally we introduce the notation $a \lesssim b$ if there exists a constant c independent of a and b, the viscosity ν and the meshsize h_T such that $a \leq cb$.

3.2. **Pressure-robust primal discretisations.** This section revisits divergence-free and pressure-robust finite element methods in a common framework. Consider an inf-sup stable pair of finite element spaces $\bar{\boldsymbol{V}}_h \subset \boldsymbol{V}$ and $\bar{Q}_h \subset Q$ and the associated discrete Stokes problem: Find $(\bar{\boldsymbol{u}}_h, \bar{p}_h) \in \bar{\boldsymbol{V}}_h \times \bar{Q}_h$ such that

$$\nu(\nabla\bar{\boldsymbol{u}}_h, \nabla\bar{\boldsymbol{v}}_h) - (\mathrm{div}(\bar{\boldsymbol{v}}_h), \bar{p}_h) = (\boldsymbol{f}, \mathcal{R}(\bar{\boldsymbol{v}}_h)) \qquad \text{for all } \bar{\boldsymbol{v}}_h \in \bar{\boldsymbol{V}}_h \tag{8a}$$

$$(\mathrm{div}(\bar{\boldsymbol{u}}_h), \bar{q}_h) = 0 \qquad \text{for all } \bar{q}_h \in \bar{Q}_h. \tag{8b}$$

Here, $\mathcal{R}$ denotes some reconstruction operator that enables pressure-robustness by mapping discretely divergence-free functions to exactly divergence-free ones. For this and in view of the expected optimal convergence rate r of the velocity ansatz space, the reconstruction operator has to satisfy, for all $\bar{\boldsymbol{v}}_h \in \bar{\boldsymbol{V}}_h, \bar{q}_h \in \bar{Q}_h$,

$$\operatorname{div}(\mathcal{R}(\bar{\boldsymbol{v}}_h)) \in \bar{Q}_h \tag{9a}$$

$$(\operatorname{div}(\bar{\boldsymbol{v}}_h), \bar{q}_h) = (\operatorname{div}(\mathcal{R}(\bar{\boldsymbol{v}}_h)), \bar{q}_h), \tag{9b}$$

$$(\boldsymbol{f}, \bar{\boldsymbol{v}}_h - \mathcal{R}(\bar{\boldsymbol{v}}_h)) = (\boldsymbol{f} - \boldsymbol{\pi}_{r-2}\boldsymbol{f}, \bar{\boldsymbol{v}}_h - \mathcal{R}(\bar{\boldsymbol{v}}_h)). \tag{9c}$$

Furthermore, for the local design of the equilibrated fluxes in Section 7, we need that the reconstruction operator does not alter continuous linear polynomials, i.e.

$$\mathcal{R}(\bar{\boldsymbol{v}}_h) = \bar{\boldsymbol{v}}_h \quad \text{for all } \bar{\boldsymbol{v}}_h \in \boldsymbol{P}_1(\mathcal{T}) \cap \boldsymbol{H}^1_0(\Omega). \tag{10}$$

Note that for discontinuous pressure discretisations all required assumptions are satisfied by the standard BDM_r interpolation operator denoted by I_{BDM_r}.

Examples for suitable finite element spaces and corresponding reconstruction operators can be found in [21, 28, 29, 31]. For any divergence-free choice, like the Scott–Vogelius (SV) finite element, no reconstruction operator is needed and one can set $\mathcal{R} = \mathbf{id}$. Table 1 lists suitable finite elements and their respective reconstruction operators that are used for our numerical experiments in Section 9. Here, $\boldsymbol{P}_{2,+}$ denotes the space of vector-valued polynomials of order 2 including the local cubic element bubbles, i.e. $\boldsymbol{P}_{2,+}(\mathcal{T}) := \{q \in \boldsymbol{P}_3(\mathcal{T}) : \forall F \in \mathcal{F}, q|_F \in \boldsymbol{P}_2(F)\}$. In three dimensions, we similarly denote by $\boldsymbol{P}^{\mathrm{3d}}_{2,+}$ the space of vector-valued polynomials of order 2 including the local element bubbles of order 4 and the cubic face bubbles of order 3. A precise definition is given in example 8.7.2 in [4]. Note that we only consider a discontinuous pressure approximation in this work since this allows an element-wise reconstruction operator, see for example [21]. However, reconstruction operators for continuous pressure approximations are also possible but demand a more complicated construction and a slightly different property (9c), see [26] for details.

The following pressure-robust a priori error estimate for the velocity can be expected, see e.g. [21] for a proof.

Theorem 3.1 (Pressure-robust a priori error estimates)**.** Assume that the velocity solution of the Stokes equations (5) fulfills the regularity $\boldsymbol{u} \in \boldsymbol{H}^m(\Omega) \cap \boldsymbol{V}_0$ with $m \geq 2$, and let $\bar{\boldsymbol{u}}_h$ be the discrete solution of (8). There holds the error estimate

$$\|\nabla(\boldsymbol{u} - \bar{\boldsymbol{u}}_h)\| \lesssim \inf_{\bar{\boldsymbol{v}}_h \in \bar{\boldsymbol{V}}_h} \|\nabla(\boldsymbol{u} - \bar{\boldsymbol{v}}_h)\| + h\|(\mathbf{id} - \boldsymbol{\pi}_{r-2})\Delta \boldsymbol{u}\| \lesssim h^s \|\boldsymbol{u}\|_{H^{s+1}}$$

where $s := \min\{m-1, r\}$.

Remark 3.2. There are also some quasi-optimal a priori error estimates under weaker regularity assumptions, see [32].

4. Drawbacks of classical equilibrated fluxes

This section discusses classical non-pressure-robust approaches which yield guaranteed upper bounds, but with deteriorating efficiency in pressure-dominant situations.

4.1. State of the art of classical non-pressure-robust flux equilibration.

In this section we shortly recall state-of-the-art equilibration error estimators for the Stokes problem from [20] in view of Theorem 2.1. For this consider the pseudo-stress reformulation of the Stokes problem

$$\widetilde{\sigma} := \nu \nabla \boldsymbol{u} - p I_{d\times d} \quad \text{and} \quad \operatorname{div} \widetilde{\sigma} + \boldsymbol{f} = 0.$$

Note that the flux $\sigma^{\text{approx}} = \widetilde{\sigma} + p I_{d\times d} = \sigma$ is equilibrated in the sense of (7) and in fact is the optimal choice for estimating the error between $\boldsymbol{u}$ and any approximation $\boldsymbol{u}^{\text{approx}} = \bar{\boldsymbol{u}}_h$ in the sense of Theorem 2.1. However, since $\boldsymbol{u}$ and p are unknown one can instead approximate discrete pseudo stress variants like

$$\widetilde{\sigma}_h = \nu \nabla \bar{\boldsymbol{u}}_h - q_2 I_{d\times d} \quad \text{and} \quad \boldsymbol{f} - \nabla q_1 + \operatorname{div}(\widetilde{\sigma}_h + q_2 I_{d\times d}) = 0$$

with (pressure approximations) $q_1 \in H^1(\Omega)$ or $q_2 \in L^2(\Omega)$. For the approximation of $\widetilde{\sigma}_h$ one can employ standard mixed methods for Poisson problems, see e.g. Remark 4.2. In practise one resorts to the choices $q_1 = 0$ and $q_2 = \bar{p}_h$ (see e.g. [20, Theorem 4.1]) or to $q_1 = \bar{p}_h \in H^1(\Omega)$ and $q_2 = 0$ (see e.g. [20, Corollary 5.1]). The following theorem summarizes the resulting error estimators.

Theorem 4.1. Consider the discrete Stokes solution $(\bar{\boldsymbol{u}}_h, \bar{p}_h) \in \boldsymbol{H}^1_0(\Omega) \times L^2_0(\Omega)$ of an inf-sup stable discretisation on some triangulation $\mathcal{T}$ with inf-sup constant $c_0 > 0$ and its discrete stress $\bar{\sigma}_h := \nu \nabla \bar{\boldsymbol{u}}_h$. For any (pseudo-stress approximation) $\widetilde{\sigma}_h \in H(\mathrm{div}, \Omega)$ with

$$\int_T \boldsymbol{f} - \nabla q_1 + \mathrm{div}(\widetilde{\sigma}_h)\,\mathrm{d}x = 0 \quad \text{for all } T \in \mathcal{T} \tag{11}$$

and some $q_1 \in H^1(\Omega)$ and $q_2 \in L^2(\Omega)$, it holds $\|\nabla \boldsymbol{u} - \nabla \bar{\boldsymbol{u}}_h\| \leq \widetilde{\eta}(\widetilde{\sigma}_h)$ with the estimator

$$\widetilde{\eta}(\widetilde{\sigma}_h)^2 \leq \nu^{-2} \sum_{T \in \mathcal{T}} \Big(\frac{h_T}{\pi} \|\boldsymbol{f} - \nabla q_1 + \mathrm{div}(\widetilde{\sigma}_h)\|_T + \|\widetilde{\sigma}_h + q_2 I_{d\times d} - \bar{\sigma}_h\|_T \Big)^2 + c_0^{-2} \|\mathrm{div}(\bar{\boldsymbol{u}}_h)\|^2.$$

Proof. The point of departure is the well-known error split [2, 20, 8]

$$\|\nabla \boldsymbol{u} - \nabla \bar{\boldsymbol{u}}_h\|^2 \leq \nu^{-2} \|\boldsymbol{r}\|^2_{\boldsymbol{V}_0^\star} + c_0^{-2} \|\mathrm{div}(\bar{\boldsymbol{u}}_h)\|^2$$

with the dual norm $\|\boldsymbol{r}\|_{\boldsymbol{V}_0^\star} := \sup_{\boldsymbol{v} \in \boldsymbol{V}_0 \setminus \{0\}} \boldsymbol{r}(\boldsymbol{v}) / \|\nabla \boldsymbol{v}\|$ of the residual

$$\boldsymbol{r}(\boldsymbol{v}) = (\boldsymbol{f}, \boldsymbol{v}) - (\bar{\sigma}_h, \nabla \boldsymbol{v}) = (\boldsymbol{f} + \mathrm{div}(\widetilde{\sigma}_h), \boldsymbol{v}) + (\widetilde{\sigma}_h - \bar{\sigma}_h, \nabla \boldsymbol{v}).$$

Due to $(\nabla q_1, \boldsymbol{v}) = 0$, we can add ∇q_1 under the first integral and then (11) allows to subtract the best-approximation $\boldsymbol{\pi}_0 \boldsymbol{v}$ into $\boldsymbol{P}_0(\mathcal{T})$ of $\boldsymbol{v}$ in the first term and employ piece-wise Poincaré inequalities to obtain

$$\begin{aligned}
(\boldsymbol{f} - \nabla q_1 + \mathrm{div}(\widetilde{\sigma}_h), \boldsymbol{v}) &= (\boldsymbol{f} - \nabla q_1 + \mathrm{div}(\widetilde{\sigma}_h), \boldsymbol{v} - \boldsymbol{\pi}_0 \boldsymbol{v}) \\
&\leq \sum_{T \in \mathcal{T}} \|\boldsymbol{f} - \nabla q_1 + \mathrm{div}(\widetilde{\sigma}_h)\|_T \|\boldsymbol{v} - \boldsymbol{\pi}_0 \boldsymbol{v}\|_T \\
&\leq \sum_{T \in \mathcal{T}} \frac{h_T}{\pi} \|\boldsymbol{f} - \nabla q_1 + \mathrm{div}(\widetilde{\sigma}_h)\|_T \|\nabla \boldsymbol{v}\|_T.
\end{aligned}$$

Since $(q_2 I_{d\times d}, \nabla \boldsymbol{v}) = 0$, the second term is estimated by

$$(\widetilde{\sigma}_h - \bar{\sigma}_h, \nabla \boldsymbol{v}) = (\widetilde{\sigma}_h + q_2 I_{d\times d} - \bar{\sigma}_h, \nabla \boldsymbol{v}) \leq \sum_{T \in \mathcal{T}} \|\widetilde{\sigma}_h + q_2 I_{d\times d} - \bar{\sigma}_h\|_T \|\nabla \boldsymbol{v}\|_T.$$

A Cauchy inequality concludes the proof. □

Remark 4.2 (Realisations)**.** A possible design of $\widetilde{\sigma}_h$ involves the Raviart-Thomas or Brezzi-Douglas-Marini finite element spaces of order k which is denoted here by $\widetilde{\boldsymbol{V}}_h$ and its divergence space denoted by $\widetilde{Q}_h$. Then one computes $\widetilde{\sigma}_h = \widetilde{\sigma}_h^{\mathsf{CEQ}} \in (\widetilde{\boldsymbol{V}}_h)^d$ and $\widetilde{\boldsymbol{u}}_h \in (\widetilde{Q}_h)^d$ such that

$$\begin{aligned}
(\widetilde{\sigma}_h^{\mathsf{CEQ}}, \tau_h) + (\boldsymbol{u}_h, \mathrm{div}(\tau_h)) &= (\bar{\sigma}_h - q_2 I_{d\times d}, \tau_h) && \text{for all } \tau_h \in (\widetilde{\boldsymbol{V}}_h)^d \\
(\boldsymbol{v}_h, \nu\, \mathrm{div}(\widetilde{\sigma}_h^{\mathsf{CEQ}})) &= -(\boldsymbol{f} - \nabla q_1, \boldsymbol{v}_h) && \text{for all } \boldsymbol{v}_h \in (\widetilde{Q}_h)^d
\end{aligned}$$

As stated above, one usually takes the discrete pressure $(q_1, q_2) = (\bar{p}_h, 0)$ or $(q_1, q_2) = (0, \bar{p}_h)$ depending on its regularity, which also enables local designs of equilibrated fluxes as detailed in e.g. [20] or using component-wise designs known for elliptic problems, see e.g. [11, 33, 5, 12, 39, 35, 15].

Remark 4.3 (Efficiency)**.** In the numerical example below, we show that even the best-approximation strategy from the previous Remark (which gives a lower bound for any local equilibration in the same space) with $q_1 = 0$ and $q_2 = \bar{p}_h$ is not efficient for the velocity error alone in a pressure-dominant situation.

Note that this is not in contradiction with efficiency proofs for these classical equilibration designs which usually focus on the error of a combined velocity-pressure norm like $\|\nabla(\boldsymbol{u} - \boldsymbol{u}_h)\| + \nu^{-1}\|p - p_h\|$ (see e.g. [20, Theorem 6.1]). Recall that pressure-robust methods allow for a velocity error that is independent of the pressure, while in classical non-pressure-robust methods the velocity error can scale with the pressure best-approximation error

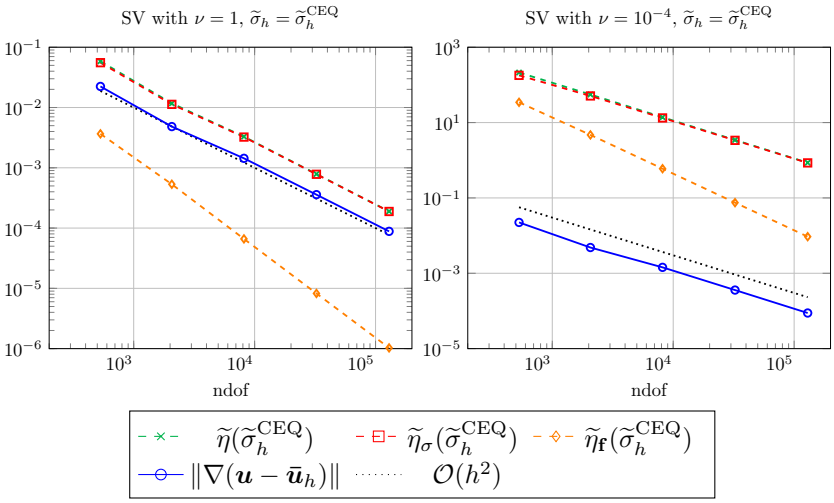

FIGURE 1. Convergence history of the exact error and the classical error estimator quantities on uniformly refined meshes for SV with $\nu = 1$ (left) and 10^{-4} (right).

in pressure-dominant situations. In such a situation, the classical error estimator, when applied to a pressure-robust method, will still be efficient for measuring the dominating pressure error, but not for the (much smaller) velocity error. As the efficiency of equilibration error estimators is usually traced back to the efficiency of the explicit estimator, the interested reader can find a deeper discussion in [27] for classical explicit standard-residual estimators.

One way to possibly improve efficiency in these pressure-dependent designs is the pre-computation of a better pressure approximation q_2 as it has been suggested e.g. in [30]. However, in situations were the pressure is complicated or non-smooth this comes at highly increased numerical costs.

4.2. **Numerical example.** In the following we demonstrate a possible deterioration of the efficiency of classical equilibration estimators even in the case of very smooth but pressure-dominant solutions. To this end we consider the Stokes problem on a unit square domain $\Omega = (0,1)^2$ with the smooth prescribed solution

$$\boldsymbol{u}(x,y) := \operatorname{curl}\left(x^2(1-x)^2y^2(1-y)^2\right) \quad \text{and} \quad p(x,y) := x^5 + y^5 - 1/3$$

with matching right-hand side $\boldsymbol{f} := -\nu\Delta\boldsymbol{u} + \nabla p$ for variable viscosity ν.

We denote by η^{CEQ} the estimator of Theorem 4.1 where $\widetilde{\sigma}_h = \widetilde{\sigma}_h^{\mathsf{CEQ}}$ is the solution of the mixed system given in Remark 4.2 with $q_1 = 0$ and $q_2 = \bar{p}_h$. Further we introduce the following quantities

$$\widetilde{\eta}_{\mathbf{f}}(\widetilde{\sigma}_h^{\mathsf{CEQ}}) := (\nu\pi)^{-1}\|h_T(\mathbf{f} + \operatorname{div}(\widetilde{\sigma}_h^{\mathsf{CEQ}}))\|,$$
$$\widetilde{\eta}_{\sigma}(\widetilde{\sigma}_h^{\mathsf{CEQ}}) := \nu^{-1}\|\widetilde{\sigma}_h^{\mathsf{CEQ}} + \bar{p}_h I_{d\times d} - \bar{\sigma}_h\|.$$

Figure 1 shows the error convergence history for uniform refinement and a corresponding barycentric refinement for the Scott–Vogelius (SV) finite element method for two different choices of ν. Since this method shows the expected convergence order $r = 2$, we used the spaces $\widetilde{\boldsymbol{V}}_h = (\mathrm{BDM}_2)^2$ and $\widetilde{Q}_h = \boldsymbol{P}_1$ in the mixed system given in Remark 4.2. As expected, the error estimator contribution $\eta_{\mathbf{f}}^{\mathsf{CEQ}}$ is of higher order, but in a pressure-dominant scenario with $\nu = 10^{-4}$ it is, even on the finest mesh, much larger than the exact error. Also the other contribution $\eta_\sigma^{\mathsf{CEQ}}$ is much larger than the exact error and not of higher order. In fact, the efficiency index scales approximately with ν^{-1}. Note that also any local equilibrated fluxes from the same space $\widetilde{\boldsymbol{V}}_h$ will only lead to larger bounds than the best-approximation in this space that we computed here.

In summary, there are situations (when $\nu^{-1}(p - \bar{p}_h)$ is large compared to $\boldsymbol{u}$) were the classical equilibration designs cannot be considered efficient for the velocity error of a pressure-robust discretisation. Note that since

the SV finite element method provides exactly divergence-free velocity solutions, it holds $c_0^{-1}\|\operatorname{div}(\bar{\boldsymbol{u}}_h)\| = 0$ in Theorem 4.1.

5. Novel pressure-robust guaranteed upper bounds

5.1. **Motivation.** The main idea of our novel relaxed equilibration is motivated by the findings of the pressure-robust mass conserving mixed stress (MCS) method from [18, 17, 24]. In order to apply this method for an equilibration in the sense of the Prager-Synge Theorem 2.1, we need to slightly weaken the regularity assumptions of σ^{approx} and the equilibration constraint (7). To this end we define the novel function space

$$H(\operatorname{curl}\operatorname{div},\Omega) := \{\tau \in L^2(\Omega)^{d\times d} : \operatorname{div}(\tau) \in (H_0(\operatorname{div},\Omega))^\star, \operatorname{tr}(\tau) = 0\},$$

where $(H_0(\operatorname{div},\Omega))^\star$ is the dual space of $H_0(\operatorname{div},\Omega) := \{\boldsymbol{v} \in H(\operatorname{div},\Omega) : \boldsymbol{v}_n = 0 \text{ on } \partial\Omega\}$. This then allows to reformulate (7) as

$$\langle \operatorname{div}(\sigma^{\text{approx}}), \boldsymbol{v}\rangle_{H_0(\operatorname{div},\Omega)} + (\boldsymbol{f},\boldsymbol{v}) = 0 \quad \text{for all } \boldsymbol{v} \in H_0(\operatorname{div},\Omega) \text{ with } \operatorname{div}(\boldsymbol{v}) = 0, \tag{12}$$

where $\langle\cdot,\cdot\rangle_{H_0(\operatorname{div},\Omega)}$ denotes the duality pair on $H_0(\operatorname{div},\Omega)$. Following the ideas of the MCS method we continue to derive a discrete version of (12). For this we define for some given $k \geq 0$, the discrete stress and velocity space by

$$\begin{aligned}\Sigma_h &:= \big\{\tau_h \in P_k(\mathcal{T})^{d\times d} : \operatorname{tr}(\tau_h) = 0; \forall F \in \mathcal{F}(\Omega), [\![(\tau_h)_{nt}]\!] = 0\big\},\\ \boldsymbol{V}_h &:= \operatorname{RT}_k(\mathcal{T}) \cap H_0(\operatorname{div},\Omega).\end{aligned}$$

Although $\boldsymbol{V}_h \subset H_0(\operatorname{div},\Omega)$, the space Σ_h is slightly non-conforming with respect to the space $H(\operatorname{curl}\operatorname{div},\Omega)$, see [24] for details. To mimic the continuous duality pair $\langle\cdot,\cdot\rangle_{H_0(\operatorname{div},\Omega)}$ we define for all functions $\sigma_h \in \Sigma_h$ and $\boldsymbol{v}_h \in \boldsymbol{V}_h$ the bilinear form

$$\begin{aligned}\langle \operatorname{div}(\sigma_h), \boldsymbol{v}_h\rangle_{\boldsymbol{V}_h} &:= \sum_{T\in\mathcal{T}} (\operatorname{div}(\sigma_h), \boldsymbol{v}_h)_T - \sum_{F\in\mathcal{F}} ([\![(\sigma_h)_{nn}]\!], (\boldsymbol{v}_h)_n)_F\\ &= -\sum_{T\in\mathcal{T}} (\sigma_h, \nabla \boldsymbol{v}_h)_T + \sum_{F\in\mathcal{F}} ((\sigma_h)_{nt}, [\![(\boldsymbol{v}_h)_t]\!])_F,\end{aligned}$$

which can be interpreted as a distributional divergence.

This then leads to a discrete version of the relaxed equilibration (12) given by

$$(\boldsymbol{f},\boldsymbol{v}_h) + \langle \operatorname{div}(\sigma_h), \boldsymbol{v}_h\rangle_{\boldsymbol{V}_h} = 0 \quad \text{for all } \boldsymbol{v}_h \in \boldsymbol{V}_h \text{ with } \operatorname{div}(\boldsymbol{v}_h) = 0.$$

Before we derive guaranteed upper bounds for $\sigma_h \in \Sigma_h$ with this constraint in Theorem 5.2 below, some additional tools are introduced.

5.2. **Commuting interpolation operators.** In the following we employ several commuting interpolators whose properties are collected here. For this note that the operator curl has a different definition in two and three dimensions and further depends on the dimension of the quantity it is applied to. If applied to some scalar-valued quantity $\psi \in H^1(\Omega)$ it is defined by $\operatorname{curl}(\psi) := (\partial_y\psi, -\partial_x\psi)^T$. If applied to some vector-valued quantity $\boldsymbol{\psi} = (\psi_1,\psi_2) \in \boldsymbol{H}^1(\Omega)$ for $d = 2$ it reads as $\operatorname{curl}(\boldsymbol{\psi}) := \partial_x\psi_2 - \partial_y\psi_1$, and if applied to some vector-valued quantity $\boldsymbol{\psi} \in H(\operatorname{curl},\Omega)$ for $d = 3$ it reads as $\operatorname{curl}(\boldsymbol{\psi}) := \nabla\times\boldsymbol{\psi}$. Now let $I_{\boldsymbol{V}_h}$ be the standard Raviart-Thomas interpolation operator. Since the de-Rham complex (i.e. the commuting properties we aim to discuss) involves different spaces depending on the spatial dimension, we define

$$W_h := \begin{cases} P_{k+1}\cap H^1(\Omega) & \text{for } d = 2 \quad (\text{Lagrange space of order } k+1),\\ \mathcal{N}_k & \text{for } d = 3 \quad (\text{Nédélec space of order } k).\end{cases}$$

Then, for $d = 3$, the interpolation I_{W_h} is the standard Nédélec interpolation operator as in [4], and for $d = 2$ we use the (corresponding commuting) H^1-interpolation operator as given in [36].

Theorem 5.1 (Commuting interpolations)**.** Let $T \in \mathcal{T}$ be an arbitrary simplex and let $F \in \mathcal{F}$ be an arbitrary face. The operators I_{W_h} and $I_{\boldsymbol{V}_h}$ enjoy the properties:

- For $d = 2$ we have the commuting property

$$I_{\boldsymbol{V}_h} \operatorname{curl}(\psi) = \operatorname{curl}(I_{W_h}\psi) \quad \text{for all } \psi \in H^2(\Omega), \tag{13}$$

and the approximation properties

$$((\mathbf{id} - I_{W_h})\psi, q_h)_F = 0 \quad \text{for all } q_h \in P_{k-1}(F), \tag{14}$$

$$((\mathbf{id} - I_{W_h})\psi, q_h)_T = 0 \quad \text{for all } q_h \in P_{k-2}(T), \tag{15}$$

$$\|\psi - I_{W_h}\psi\|_T \leq c_2 h_T \|\nabla\psi\|_T \quad \text{for all } \psi \in H^2(T). \tag{16}$$

- For $d = 3$ we have the commuting property

$$I_{\boldsymbol{V}_h} \operatorname{curl} \boldsymbol{\psi} = \operatorname{curl}(I_{W_h}\boldsymbol{\psi}) \quad \text{for all } \boldsymbol{\psi} \in \boldsymbol{H}^1(\operatorname{curl}, \Omega), \tag{17}$$

where $\boldsymbol{H}^1(\operatorname{curl}, \Omega) = \{\boldsymbol{\psi} \in \boldsymbol{H}^1(\Omega) : \operatorname{curl}(\boldsymbol{\psi}) \in \boldsymbol{H}^1(\Omega)\}$, and the approximation properties

$$((\mathbf{id} - I_{W_h})\boldsymbol{\psi}, \boldsymbol{q}_h \times \boldsymbol{n})_F = 0 \quad \text{for all } \boldsymbol{q}_h \in \boldsymbol{P}_{k-1}(F), \tag{18}$$

$$((\mathbf{id} - I_{W_h})\boldsymbol{\psi}, \boldsymbol{q}_h)_T = 0 \quad \text{for all } \boldsymbol{q}_h \in \boldsymbol{P}_{k-2}(T), \tag{19}$$

$$\|\boldsymbol{\psi} - I_{W_h}\boldsymbol{\psi}\|_T \leq c_2 h_T \|\nabla\boldsymbol{\psi}\|_T \quad \text{for all } \boldsymbol{\psi} \in \boldsymbol{H}^1(\operatorname{curl}, T). \tag{20}$$

- For $d = 2$ and $d = 3$ we have

$$(((\mathbf{id} - I_{\boldsymbol{V}_h})\boldsymbol{v})_n,\ q_h)_F = 0 \quad \text{for all } q_h \in P_k(F), \tag{21}$$

$$((\mathbf{id} - I_{\boldsymbol{V}_h})\boldsymbol{v}, \boldsymbol{q}_h)_T = 0 \quad \text{for all } \boldsymbol{q}_h \in \mathcal{N}_{k-2}(T), \tag{22}$$

$$\|\boldsymbol{v} - I_{\boldsymbol{V}_h}\boldsymbol{v}\|_T \leq c_1 h_T \|\nabla\boldsymbol{v}\|_T \quad \text{for all } \boldsymbol{v} \in \boldsymbol{H}^1(T), \tag{23}$$

with constants c_1, c_2 independent of h_T.

Proof. The properties of I_{W_h} in two and three dimensions follows with the results in [36] and standard Bramble-Hilbert type arguments. Note that the results in [36] (in two dimensions) are only given for the rotated commuting diagram, i.e. $\nabla I_{W_h}\psi = I_{\mathcal{N}_k}(\nabla\psi)$, where $I_{\mathcal{N}_k}$ is the standard Nédélec interpolator. The claimed results in this work follow immediately as the Raviart–Thomas space is simply a rotated Nédélec space and the curl is the rotated gradient, thus we have $(I_{\mathcal{N}_k}(\nabla\psi))^\perp = I_{\boldsymbol{V}_h}(\operatorname{curl}\psi)$. Similar results can be found in [10, 34, 4].

Equation (21) is a standard property of the Raviart-Thomas interpolation operator, see e.g. [4]. We continue with the proof of (22) but only present the case $d = 3$ since the two dimensional results follows with similar arguments. First observe that any divergence-free function $\boldsymbol{v} \in \boldsymbol{V}_0$ has a (local) potential $\boldsymbol{v} = \operatorname{curl}(\boldsymbol{\psi})$ for some $\boldsymbol{\psi} \in H^1(\operatorname{curl}, T)$. Then, for any $\boldsymbol{q}_h \in \mathcal{N}_{k-2}(T)$, (17) and an integration by parts show

$$\begin{aligned}((\mathbf{id} - I_{\boldsymbol{V}_h})\boldsymbol{v}, \boldsymbol{q}_h)_T &= ((\mathbf{id} - I_{\boldsymbol{V}_h})\operatorname{curl}(\boldsymbol{\psi}), \boldsymbol{q}_h)_T = (\operatorname{curl}((\mathbf{id} - I_{W_h})\boldsymbol{\psi}), \boldsymbol{q}_h)_T \\ &= ((\mathbf{id} - I_{W_h})\boldsymbol{\psi}, \operatorname{curl}(\boldsymbol{q}_h))_T - ((\mathbf{id} - I_{W_h})\boldsymbol{\psi}, \boldsymbol{q}_h \times \boldsymbol{n})_F.\end{aligned}$$

Since $\boldsymbol{q}_h \in \mathcal{N}_{k-2}(T) \subset \mathcal{P}_{k-1}(T)$ and hence $\operatorname{curl}(\boldsymbol{q}_h) \in P_{k-2}(T)$ and $\boldsymbol{q}_h \times \boldsymbol{n}|_F \in P_{k-1}(F)$, the right-hand side vanishes due to (19) and (18). This concludes the proof. □

5.3. **Novel pressure-robust guaranteed upper bounds.** We are now in the position to derive pressure-robust guaranteed upper bounds via equilibrated fluxes with a proper discrete analogue of the equilibration constraint (7).

Theorem 5.2. Assume the regularity $\boldsymbol{f} \in H(\operatorname{curl}, \Omega)$. Let $\bar{\boldsymbol{u}}_h, \bar{p}_h$ be the solution of (8) and let $\bar{\sigma}_h := \nu\nabla\bar{\boldsymbol{u}}_h$. For any discrete stress $\sigma_h \in \Sigma_h$ that is equilibrated in the sense

$$(\boldsymbol{f}, \boldsymbol{v}_h) + \langle \operatorname{div}(\sigma_h), \boldsymbol{v}_h\rangle_{\boldsymbol{V}_h} = 0 \quad \text{for all } \boldsymbol{v}_h \in \boldsymbol{V}_h \text{ with } \operatorname{div}(\boldsymbol{v}_h) = 0, \tag{24}$$

it holds $\|\nabla(\boldsymbol{u} - \bar{\boldsymbol{u}}_h)\| \leq \eta(\sigma_h)$ with the error estimator

$$\eta(\sigma_h)^2 := \nu^{-2} \sum_{T\in\mathcal{T}} \Big(c_1 c_2 h_T^2 \|(\mathbf{id} - \boldsymbol{\pi}_{k-2})\operatorname{curl}(\boldsymbol{f})\|_T + \|\operatorname{dev}(\sigma_h - \bar{\sigma}_h)\|_T\Big)^2 + c_0^{-2}\|\operatorname{div}(\bar{\boldsymbol{u}}_h)\|^2.$$

Proof. As in Theorem 4.1 the point of departure is the error split

$$\|\nabla(\boldsymbol{u}-\bar{\boldsymbol{u}}_h)\|^2 \leq \nu^{-2}\|\boldsymbol{r}\|^2_{\boldsymbol{V}_0^\star} + c_0^{-2}\|\operatorname{div}(\bar{\boldsymbol{u}}_h)\|^2$$

where it remains to bound the residual functional

$$\boldsymbol{r}(\boldsymbol{v}) = (\boldsymbol{f},\boldsymbol{v}) - (\bar{\sigma}_h, \nabla\boldsymbol{v}) \quad \text{for all } \boldsymbol{v}\in\boldsymbol{V}_0,$$

in its dual norm

$$\|\boldsymbol{r}\|_{\boldsymbol{V}_0^\star} := \sup_{\boldsymbol{v}\in\boldsymbol{V}_0\setminus\{\boldsymbol{0}\}} \frac{\boldsymbol{r}(\boldsymbol{v})}{\|\nabla\boldsymbol{v}\|}.$$

Consider an arbitrary test function $\boldsymbol{v}\in\boldsymbol{V}_0$ and some equilibrated flux σ_h with the properties stated above. The equilibration constraint (24) for $\boldsymbol{v}_h = I_{\boldsymbol{V}_h}\boldsymbol{v}$ and an integration by parts yields

$$\begin{aligned}\boldsymbol{r}(\boldsymbol{v}) =& \langle \boldsymbol{f}+\operatorname{div}(\sigma_h), \boldsymbol{v}-I_{\boldsymbol{V}_h}\boldsymbol{v}\rangle_{\boldsymbol{V}_h} + (\sigma_h-\bar{\sigma}_h,\nabla\boldsymbol{v})\\ =& \sum_{T\in\mathcal{T}} (\boldsymbol{f}+\operatorname{div}(\sigma_h), \boldsymbol{v}-I_{\boldsymbol{V}_h}\boldsymbol{v})_T\\ &+ \sum_{F\in\mathcal{F}(\Omega)} (\llbracket(\sigma_h)_{nn}\rrbracket, (\boldsymbol{v}-I_{\boldsymbol{V}_h}\boldsymbol{v})_n)_F + (\sigma_h-\bar{\sigma}_h,\nabla\boldsymbol{v}).\end{aligned}$$

Since $\llbracket(\sigma_h)_{nn}\rrbracket \in P_k(F)$, the second integral vanishes using to orthogonality properties of the normal flux of $(\boldsymbol{v}-I_{\boldsymbol{V}_h}\boldsymbol{v})$, see (21) of Theorem 5.1. The last integral on the right-hand side can be estimated by

$$(\sigma_h-\bar{\sigma}_h,\nabla\boldsymbol{v}) = (\operatorname{dev}(\sigma_h-\bar{\sigma}_h),\nabla\boldsymbol{v}) \leq \sum_{T\in\mathcal{T}} \|\operatorname{dev}(\sigma_h-\bar{\sigma}_h)\|_T\|\nabla\boldsymbol{v}\|_T. \tag{25}$$

Here, $\operatorname{dev}(A)$ denotes the deviatoric part of a A and it was used that $A-\operatorname{dev}(A) = \operatorname{tr}(A)I_{d\times d}/d$ is orthogonal on gradients of divergence-free functions.

The estimate of the first integral will be presented only for the case $d=3$, as for $d=2$ the arguments are very similar. Since $\boldsymbol{v}-I_{\boldsymbol{V}_h}\boldsymbol{v}$ is divergence-free, there exists some $\boldsymbol{\psi}\in\boldsymbol{H}^1(\Omega)$ with $\|\nabla\boldsymbol{\psi}\|_T \leq \|\boldsymbol{v}-I_{\boldsymbol{V}_h}\boldsymbol{v}\|_T$, see for example in [9], such that $\boldsymbol{v}-I_{\boldsymbol{V}_h}\boldsymbol{v} = \operatorname{curl}\boldsymbol{\psi}$ and by the interpolation properties we have

$$\|\nabla\boldsymbol{\psi}\|_T \leq \|\operatorname{curl}\boldsymbol{\psi}\|_T = \|\boldsymbol{v}-I_{\boldsymbol{V}_h}\boldsymbol{v}\|_T \leq c_1 h_T\|\nabla\boldsymbol{v}\|_T \quad \text{on every } T\in\mathcal{T}. \tag{26}$$

Moreover, it holds $I_{\boldsymbol{V}_h}\operatorname{curl}\boldsymbol{\psi}=0$ and hence, the commuting property (17) in Theorem 5.1 yields $\operatorname{curl} I_{W_h}\boldsymbol{\psi}=0$ where I_{W_h} is the matching commuting interpolation operator. Note that the application of the operator I_{W_h} to $\boldsymbol{\psi}$ is well defined, since locally on each element $T\in\mathcal{T}$ we have that $\boldsymbol{v}-I_{\boldsymbol{V}_h}\boldsymbol{v}\in\boldsymbol{H}^1(T)$ and thus we can bound $\|\nabla\operatorname{curl}\boldsymbol{\psi}\|_T \leq \|\nabla(\boldsymbol{v}-I_{\boldsymbol{V}_h}\boldsymbol{v})\|_T$ which gives $\boldsymbol{\psi}\in\boldsymbol{H}^1(\operatorname{curl},T)$.

Next, if $k\geq 2$, consider some Nédélec function $\boldsymbol{\theta}_h\in\mathcal{N}_{k-2}(\mathcal{T})$ chosen such that $\operatorname{curl}\boldsymbol{\theta}_h = \boldsymbol{\pi}_{k-2}\operatorname{curl}(\boldsymbol{f}+\operatorname{div}(\sigma_h))$. Then, (22) and the properties of σ_h yield

$$\begin{aligned}\sum_{T\in\mathcal{T}} (\boldsymbol{f}+\operatorname{div}(\sigma_h), \boldsymbol{v}-I_{\boldsymbol{V}_h}\boldsymbol{v})_T &= \sum_{T\in\mathcal{T}} (\boldsymbol{f}+\operatorname{div}(\sigma_h)-\boldsymbol{\theta}_h, \operatorname{curl}(\boldsymbol{\psi}-I_{W_h}\boldsymbol{\psi}))_T\\ &= \sum_{T\in\mathcal{T}} (\mathbf{id}-\boldsymbol{\pi}_{k-2})\operatorname{curl}(\boldsymbol{f}+\operatorname{div}(\sigma_h)), \boldsymbol{\psi}-I_{W_h}\boldsymbol{\psi})_T\\ &\quad + \sum_{F\in\mathcal{F}(\Omega)} (\llbracket\boldsymbol{f}+\operatorname{div}(\sigma_h)\rrbracket\times\boldsymbol{n}, \boldsymbol{\psi}-I_{W_h}\boldsymbol{\psi})_F.\end{aligned}$$

Since $\boldsymbol{f}\in H(\operatorname{curl},\Omega)$ and $\operatorname{div}(\sigma_h)\in\boldsymbol{P}_{k-1}(\mathcal{T})$, the second integral vanishes due to property (18) of I_{W_h} from Theorem 5.1. For the remaining term the equation $(\mathbf{id}-\boldsymbol{\pi}_{k-2})\operatorname{curl}(\operatorname{div}(\sigma_h))=0$, the interpolation properties

of I_{W_h} (see again Theorem 5.1) and (26) yield

$$\begin{aligned}\sum_{T\in\mathcal{T}}((\mathbf{id}-\boldsymbol{\pi}_{k-2})\operatorname{curl}(\boldsymbol{f}+\operatorname{div}(\sigma_h)),\boldsymbol{\psi}-I_{W_h}\boldsymbol{\psi})_T&\\ \leq\sum_{T\in\mathcal{T}}\|(\mathbf{id}-\boldsymbol{\pi}_{k-2})\operatorname{curl}(\boldsymbol{f})\|_T\|\boldsymbol{\psi}-I_{W_h}\boldsymbol{\psi}\|_T&\\ \leq\sum_{T\in\mathcal{T}}c_2h_T\|(\mathbf{id}-\boldsymbol{\pi}_{k-2})\operatorname{curl}(\boldsymbol{f})\|_T\|\nabla\boldsymbol{\psi}\|_T&\\ \leq\sum_{T\in\mathcal{T}}c_1c_2h_T^2\|(\mathbf{id}-\boldsymbol{\pi}_{k-2})\operatorname{curl}(\boldsymbol{f})\|_T\|\nabla\boldsymbol{v}\|_T.&\end{aligned}$$

The last estimate, (25) and a Cauchy inequality show

$$\boldsymbol{r}(\boldsymbol{v})\leq\sum_{T\in\mathcal{T}}\Big(c_1c_2h_T^2\|(\mathbf{id}-\boldsymbol{\pi}_{k-2})\operatorname{curl}(\boldsymbol{f})\|_T+\|\operatorname{dev}(\sigma_h-\bar\sigma_h)\|_T\Big)\|\nabla\boldsymbol{v}\|_T$$

and hence

$$\|\boldsymbol{r}\|_{\boldsymbol{V}_0^\star}^2\leq\sum_{T\in\mathcal{T}}\Big(c_1c_2h_T^2\|(\mathbf{id}-\boldsymbol{\pi}_{k-2})\operatorname{curl}(\boldsymbol{f})\|_T+\|\operatorname{dev}(\sigma_h-\bar\sigma_h)\|_T\Big)^2.$$

This concludes the proof. □

Remark 5.3. Theorem 5.2 also holds true in the case when we only have the local regularity assumption $\boldsymbol{f}\in H(\operatorname{curl},T)$ for all $T\in\mathcal{T}$. Note however, that this introduces another term on the boundary of the elements given by

$$c_3\sum_{F\in\mathcal{F}(\Omega)}h_F^3\|(\mathbf{id}-\boldsymbol{\pi}_{k-1})[\![\boldsymbol{f}\times\boldsymbol{n}]\!]\|_F^2$$

added to the estimator $\eta(\sigma_h)^2$ given in Theorem 5.2. Here, c_3 is an additional constant that only depends on the shape of the simplices $T\in\mathcal{T}$.

Remark 5.4 (Divergence error)**.** In the numerical examples of Section 9 it becomes apparent that the efficiency of the error estimator is mostly limited by the divergence-term $c_0^{-1}\|\operatorname{div}(\boldsymbol{u}_h)\|$ for non-divergence-free discretisations. To avoid this term and possibly further increase the efficiency, one may consider a divergence-free post-processing $\boldsymbol{s}_h\in\boldsymbol{H}^1(\Omega)$ of $\boldsymbol{u}_h$ and perform the error estimation for $\boldsymbol{s}_h$ or $\bar\sigma_h:=\nabla\boldsymbol{s}_h$. Effectively this would replace the term $c_0^{-1}\|\operatorname{div}(\boldsymbol{u}_h)\|$ by $\|\nabla(\boldsymbol{s}_h-\bar{\boldsymbol{u}}_h)\|$ without the possibly small constant c_0. A candidate for such a post-processing may be a locally computed approximation into a divergence-free Scott–Vogelius finite element space (on a barycentrically refined subgrid) similar to [23].

6. Global Equilibration

This section derives one possible design of an equilibrated flux $\sigma_h=\sigma_h^{\mathsf{GEQ}}$ for Theorem 5.2. The idea is to solve a global problem with a mixed MCS method: Find $(\sigma_h^{\mathsf{GEQ}},\boldsymbol{u}_h,p_h)\in\Sigma_h\times\boldsymbol{V}_h\times Q_h$ such that

$$\frac{1}{\nu}(\sigma_h^{\mathsf{GEQ}},\tau_h)+\langle\operatorname{div}(\tau_h),\boldsymbol{u}_h\rangle_{\boldsymbol{V}_h}=(\nabla\bar{\boldsymbol{u}}_h,\tau_h)\qquad\text{for all }\tau_h\in\Sigma_h,\tag{27a}$$

$$\langle\operatorname{div}(\sigma_h^{\mathsf{GEQ}}),\boldsymbol{v}_h\rangle_{\boldsymbol{V}_h}+(\operatorname{div}(\boldsymbol{v}_h),p_h)=(-\boldsymbol{f},\boldsymbol{v}_h)\qquad\text{for all }\boldsymbol{v}_h\in\boldsymbol{V}_h,\tag{27b}$$

$$(\operatorname{div}(\boldsymbol{u}_h),q_h)=-(\operatorname{div}(\bar{\boldsymbol{u}}_h),q_h)\qquad\text{for all }q_h\in Q_h.\tag{27c}$$

The system (27) can be interpreted as an L^2-minimization problem with constraints given by

$$\|\sigma_h^{\mathsf{GEQ}}-\nu\nabla\bar{\boldsymbol{u}}_h\|_{L^2(\Omega)}\to\min\quad\text{such that}\quad\langle\operatorname{div}(\sigma_h),I_{\boldsymbol{V}_h}\boldsymbol{V}_0\rangle_{\boldsymbol{V}_h}=(-\boldsymbol{f},I_{\boldsymbol{V}_h}\boldsymbol{V}_0).$$

Since no explicit basis for $I_{\boldsymbol{V}_h}\boldsymbol{V}_0$ (i.e. exactly divergence-free Raviart-Thomas functions) can be constructed, the divergence constraint is employed by means of the Lagrange multiplier p_h.

Theorem 6.1. The solution σ_h^{GEQ} of problem (27) satisfies the discrete equilibration constraint (24). If the exact velocity solution of 5 fulfills the regularity $\boldsymbol{u} \in \boldsymbol{H}^m(\mathcal{T}) \cap \boldsymbol{V}_0$ with $m \geq 2$, it holds the error estimate

$$\|\sigma - \sigma_h^{\mathsf{GEQ}}\| \lesssim h^s \nu \|\boldsymbol{u}\|_{H^{s+1}(\mathcal{T})}$$

where $s := \min\{m-1, k+1\}$ and $\sigma = \nu \nabla \boldsymbol{u}$.

Proof. The equilibration constraint follows from the second equation of the discrete system (27), since given any $\boldsymbol{v} \in \boldsymbol{V}_0$, testing with the divergence-free function $\boldsymbol{v}_h := I_{\boldsymbol{V}_h} \boldsymbol{v}$ leads to $\langle \operatorname{div}(\sigma_h^{\mathsf{GEQ}}), \boldsymbol{v}_h \rangle_{\boldsymbol{V}_h} = (-\boldsymbol{f}, \boldsymbol{v}_h)$.

We continue with the error estimate by showing that the solution of the best-approximation problem (27) is related to solving a MCS-Stokes problem with a zero right-hand in the first and third equation. To this end let $\boldsymbol{w}_h = \boldsymbol{u}_h + I_{\boldsymbol{V}_h} \bar{\boldsymbol{u}}_h$. Since $\operatorname{div}(\tau_h) \in P_{k-1}(T)^2$ for all $T \in \mathcal{T}$ and $[\![(\tau_h)_{nn}]\!] \in P_k(F)$ for all $F \in \mathcal{F}$, the properties of the Raviart-Thomas interpolator, integration by parts and the H^1-continuity of $\bar{\boldsymbol{u}}_h$ give

$$\begin{aligned}
\langle \operatorname{div}(\tau_h), I_{\boldsymbol{V}_h} \bar{\boldsymbol{u}}_h \rangle_{\boldsymbol{V}_h} &= \sum_{T \in \mathcal{T}} (\operatorname{div}(\tau_h), I_{\boldsymbol{V}_h} \bar{\boldsymbol{u}}_h)_T - \sum_{F \in \mathcal{F}} ([\![(\tau_h)_{nn}]\!], (I_{\boldsymbol{V}_h} \bar{\boldsymbol{u}}_h)_n)_F \\
&= \sum_{T \in \mathcal{T}} (\operatorname{div}(\tau_h), \bar{\boldsymbol{u}}_h)_T - \sum_{F \in \mathcal{F}} ([\![(\tau_h)_{nn}]\!], (\bar{\boldsymbol{u}}_h)_n)_F \\
&= -\sum_{T \in \mathcal{T}} (\tau_h, \nabla \bar{\boldsymbol{u}}_h)_T + \sum_{F \in \mathcal{F}} ((\tau_h)_{nt}, [\![(\bar{\boldsymbol{u}}_h)_t]\!])_F \\
&= -(\nabla \bar{\boldsymbol{u}}_h, \tau_h).
\end{aligned}$$

Further we have $(\operatorname{div}(I_{\boldsymbol{V}_h} \bar{\boldsymbol{u}}_h), q_h) = (\operatorname{div}(\bar{\boldsymbol{u}}_h), q_h)$ for all $q_h \in Q_h$. This shows that the triplet $(\sigma_h^{\mathsf{GEQ}}, \boldsymbol{w}_h, p_h) \in \Sigma_h \times \boldsymbol{V}_h \times Q_h$ solves the problem

$$\begin{aligned}
\frac{1}{\nu}(\sigma_h^{\mathsf{GEQ}}, \tau_h) + \langle \operatorname{div}(\tau_h), \boldsymbol{w}_h \rangle_{\boldsymbol{V}_h} &= 0 && \text{for all } \tau_h \in \Sigma_h, \\
\langle \operatorname{div}(\sigma_h^{\mathsf{GEQ}}), \boldsymbol{v}_h \rangle_{\boldsymbol{V}_h} + (\operatorname{div}(\boldsymbol{v}_h), p_h) &= (-\boldsymbol{f}, \boldsymbol{v}_h) && \text{for all } \boldsymbol{v}_h \in \boldsymbol{V}_h, \\
(\operatorname{div}(\boldsymbol{w}_h), q_h) &= 0 && \text{for all } q_h \in Q_h.
\end{aligned}$$

Since $\boldsymbol{w}_h \in \boldsymbol{V}_h$ is exactly divergence-free, the pressure-robust error estimates of the standard Stokes problem (discretised by the MCS method) from [24, 17] give

$$\|\sigma - \sigma_h^{\mathsf{GEQ}}\| \lesssim h^s \nu \|\boldsymbol{u}\|_{H^{s+1}}.$$

This concludes the proof. □

The following theorem proves global efficiency of the global design.

Theorem 6.2 (Global efficiency of the global design)**.** The error estimator for $\sigma_h := \sigma_h^{\mathsf{GEQ}}$ from (27), is efficient in the sense that

$$\eta(\sigma_h^{\mathsf{GEQ}}) \lesssim \nu^{-1} \Big(\|\sigma - \bar{\sigma}_h\| + \|\sigma - \sigma_h^{\mathsf{GEQ}}\| + \operatorname{osc}_{k-2}(\operatorname{curl}(\boldsymbol{f})) \Big),$$

with the data oscillations

$$\operatorname{osc}_{k-2}(\operatorname{curl}(\boldsymbol{f})) := \Big(\sum_{T \in \mathcal{T}} h_T^2 \|(\mathbf{id} - \boldsymbol{\pi}_{k-2}) \operatorname{curl}(\boldsymbol{f})\|_T^2 \Big)^{1/2}. \tag{28}$$

Note that the oscillations and the second term on the right-hand side (estimated in Theorem 6.1) are of order h_T^{k+1} if the data is smooth enough.

Proof. This follows by the definition of the estimator η of Theorem 5.2 and the triangle inequality

$$\|\operatorname{dev}(\sigma_h - \bar{\sigma}_h)\| \leq \|\sigma_h - \bar{\sigma}_h\| \leq \|\sigma - \bar{\sigma}_h\| + \|\sigma - \sigma_h\|,$$

and the estimate

$$\|\operatorname{div}(\bar{\boldsymbol{u}}_h)\| = \|\operatorname{div}(u - \bar{\boldsymbol{u}}_h)\| \leq \nu^{-1} \|\sigma - \bar{\sigma}_h\|.$$

□

7. Local Equilibration

This section suggests some design of an admissible pressure-robust equilibrated flux $\sigma_h = \sigma_h^{\mathsf{LEQ}}$ for Theorem 5.2 based on local problems on vertex patches.

7.1. **Setup of the local problems.** Let $\mathcal{V}$ be the set of vertices of a triangulation $\mathcal{T}$. For $V \in \mathcal{V}$ let ω_V denote the corresponding vertex patch, i.e. the union of all adjacent cells in $\mathcal{T}_V := \{T \in \mathcal{T} : V \in \overline{T}\}$. Furthermore, $\mathcal{F}_V$ denotes the set of facets within the vertex patch including the facets on the boundary $\partial\omega_V$. For a fixed interior vertex V we define the following spaces with $k = r$ (recall that r is the optimal convergence rate of the primal method)

$$\begin{aligned}
\Sigma_h^V &:= \{\tau_h \in L^2(\mathcal{T}_V)^{d\times d} : \forall T \in \mathcal{T}_V,\ \tau_h|_T \in P_k(T)^{d\times d} \text{ with } \mathrm{tr}(\tau_h) = 0\},\\
\boldsymbol{V}_h^V &:= \mathrm{RT}_k(\mathcal{T}_V),\\
\hat{\boldsymbol{V}}_h^V &:= \{\hat{\boldsymbol{v}}_h \in \boldsymbol{L}^2(\mathcal{F}_V) : \forall F \in \mathcal{F}_V,\ \hat{\boldsymbol{v}}_h|_F \in \boldsymbol{P}_k(F) \text{ and } (\hat{\boldsymbol{v}}_h)_n = 0\},\\
Q_h^V &:= \{q_h \in L^2(\mathcal{T}_V) : \forall T \in \mathcal{T}_V,\ q_h|_T \in P_k(T)\}.
\end{aligned}$$

Note that in contrast to the global stress space Σ_h, the local stress space Σ_h^V is broken, i.e., does not include the continuity constraint $[\![(\tau_h)_{nt}]\!] = 0$. Similarly to other local equilibration setups, see for example [5], the space $\hat{\boldsymbol{V}}_h^V$ is chosen such that the normal-tangential trace of functions in Σ_h^V lie in $\hat{\boldsymbol{V}}_h^V$.

For the local problems we then further define the product space

$$\boldsymbol{X}_h^V := (\boldsymbol{V}_h^V \times \hat{\boldsymbol{V}}_h^V)/\{(\boldsymbol{c}, \boldsymbol{c}_t) : \boldsymbol{c} \in \mathbb{R}^d\}, \tag{29}$$

where $\boldsymbol{c}$ denotes a vector-valued constant, and $(\boldsymbol{c}, \boldsymbol{c}_t)$ reads as (a constant) element of the product space $\boldsymbol{V}_h^V \times \hat{\boldsymbol{V}}_h^V$. Hence, the space $\boldsymbol{X}_h^V$ is factorised by vector-valued constant functions on the patch.

The projection onto vector-valued constants $\boldsymbol{\pi}_{\mathbb{R}}^V : \boldsymbol{L}^2(\mathcal{T}_V) \times [\boldsymbol{L}^2(\mathcal{F}_V)]_t \to \mathbb{R}^d$ is given by

$$\boldsymbol{\pi}_{\mathbb{R}}^V(\boldsymbol{v}_h, \hat{\boldsymbol{v}}_h) := \frac{1}{|\mathcal{T}_V| + |\mathcal{F}_V|}\Big(\sum_{T\in\mathcal{T}_V}\int_T \boldsymbol{v}_h \,\mathrm{d}x + \sum_{F\in\mathcal{F}_V}\int_F \hat{\boldsymbol{v}}_h \,\mathrm{d}s\Big) \in \mathbb{R}^d.$$

Here the quantities $|\mathcal{T}_V|$ and $|\mathcal{F}_V|$ denote the area of the element patch and the skeleton of the patch respectively. Note that we then have the equality

$$\boldsymbol{X}_h^V = \{(\boldsymbol{v}_h, \hat{\boldsymbol{v}}_h) \in \boldsymbol{V}_h^V \times \hat{\boldsymbol{V}}_h^V : (\mathbf{id} - \boldsymbol{\pi}_{\mathbb{R}}^V)(\boldsymbol{v}_h, \hat{\boldsymbol{v}}_h) \neq \mathbf{0}\}. \tag{30}$$

For each element $T \in \mathcal{T}$ and every vertex $V \in T$ we define the scalar linear operator

$$B_T^V : P_{k+1}(T) \to P_k(T),\ v_h \mapsto B_T^V(v_h) := I_{\mathcal{L}}^k(\phi_V v_h),$$

where $I_{\mathcal{L}}^k$ denotes the nodal (Lagrange) interpolation operator into $P_k(T)$ and ϕ_V is the hat function of the vertex V. By that we then define on ω_V the scalar bubble projector (see also [26])

$$B^V : P_{k+1}(\mathcal{T}_V) \to P_k(\mathcal{T}_V),\ v_h \mapsto B^V(v_h) := \sum_{T\in\mathcal{T}_V} B_T^V(v_h),$$

and the (vector-valued) bubble projector

$$\boldsymbol{B}^V : \boldsymbol{P}_{k+1}(\mathcal{T}_V) \to \boldsymbol{P}_k(\mathcal{T}_V),\ \boldsymbol{v}_h \mapsto \boldsymbol{B}^V(\boldsymbol{v}_h) \quad \text{with} \quad (\boldsymbol{B}^V(\boldsymbol{v}_h))_j := B^V((\boldsymbol{v}_h)_j),$$

where $(\cdot)_j$ denotes the j-th component of the vector.

Lemma 7.1. The bubble projector $\boldsymbol{B}^V$ fulfills the following properties:

i. $\boldsymbol{B}^V(\boldsymbol{v}_h)|_{\partial\omega_V} = 0$ for all $\boldsymbol{v}_h \in \boldsymbol{V}_h^V$
ii. Let $\boldsymbol{v}_h^V \in \boldsymbol{V}_h^V$ then $\boldsymbol{B}^V(\boldsymbol{v}_h^V) \in \mathrm{BDM}_k(\mathcal{T}_V)$.

iii. For all elements $T \in \mathcal{T}$ we have the partition of unity property

$$\sum_{V \in T} \boldsymbol{B}^V(\boldsymbol{v}_h|_T) = \boldsymbol{v}_h|_T \quad \text{for all } \boldsymbol{v}_h \in \boldsymbol{V}_h \text{ with } \operatorname{div}(\boldsymbol{v}_h) = 0.$$

iv. For a constant $\boldsymbol{c} \in \mathbb{R}^d$ there holds $\boldsymbol{B}^V(\boldsymbol{c}) = \phi_V \boldsymbol{c}$.

Proof. Item i. follows by the definition and the linearity of the bubble projection. For the proof of ii. choose an arbitrary edge $F \in \mathcal{F}_V$ with the corresponding normal vector $\boldsymbol{n}$. Since $\boldsymbol{v}_h^V$ is normal continuous we have by the properties of the nodal interpolation operator that

$$[\![(\boldsymbol{B}^V(\boldsymbol{v}_h^V)(\boldsymbol{x}))_n]\!] = \phi_V(\boldsymbol{x})[\![(\boldsymbol{v}_h^V(\boldsymbol{x}))_n]\!] = 0 \quad \text{for all } \boldsymbol{x} \in F.$$

This shows that $\boldsymbol{B}^V(\boldsymbol{v}_h^V)$ is normal continuous and as $\boldsymbol{B}^V(\boldsymbol{v}_h^V) \in \boldsymbol{P}_k(\mathcal{T}_V)$ it follows that $\boldsymbol{B}^V(\boldsymbol{v}_h^V) \in \mathrm{BDM}_k(\mathcal{T}_V)$. For iii. let $\boldsymbol{v}_h \in \boldsymbol{V}_h$ with $\operatorname{div}(\boldsymbol{v}_h) = 0$ be arbitrary. Since $\boldsymbol{v}_h$ is divergence-free it follows that $\boldsymbol{v}_h \in \mathrm{BDM}_k(\mathcal{T})$, thus $\boldsymbol{v}_h|_T \in \boldsymbol{P}_k(T)$ and so $I_{\mathcal{L}}^k(\boldsymbol{v}_h|_T) = \boldsymbol{v}_h|_T$. The claimed partition of unity property then follows by the linearity of the bubble projector $\boldsymbol{B}^V$. The last item iv. follows for each component separately since there holds $I_{\mathcal{L}}^k(c\phi_V) = c\phi_V$ on each element $T \in \mathcal{T}_V$ and all $c \in \mathbb{R}$. This concludes the proof. □

For each vertex V we solve the local problem: Find $(\sigma_h^V, (\boldsymbol{u}_h^V, \hat{\boldsymbol{u}}_h^V), p_h^V) \in \Sigma_h^V \times \boldsymbol{X}_h^V \times Q_h^V$ such that, for all $(\tau_h^V, (\boldsymbol{v}_h^V, \hat{\boldsymbol{v}}_h^V), q_h^V) \in \Sigma_h^V \times \boldsymbol{X}_h^V \times Q_h^V$,

$$(\sigma_h^V, \tau_h^V)_{\omega_V} + \langle \operatorname{div}(\tau_h^V), (\boldsymbol{u}_h^V, \hat{\boldsymbol{u}}_h^V)\rangle_{\boldsymbol{V}_h^V} = 0 \tag{31a}$$

$$\langle \operatorname{div}(\sigma_h^V), (\boldsymbol{v}_h^V, \hat{\boldsymbol{v}}_h^V)\rangle_{\boldsymbol{V}_h^V} + (\operatorname{div}(\boldsymbol{v}_h^V), p_h^V)_{\omega_V} = \boldsymbol{r}^V((\boldsymbol{v}_h^V, \hat{\boldsymbol{v}}_h^V)), \tag{31b}$$

$$(\operatorname{div}(\boldsymbol{u}_h^V), q_h^V)_{\omega_V} = 0, \tag{31c}$$

with the bilinear form

$$\begin{aligned}\langle \operatorname{div}(\tau_h^V), (\boldsymbol{u}_h^V, \hat{\boldsymbol{u}}_h^V)\rangle_{\boldsymbol{V}_h^V} := &\sum_{T \in \mathcal{T}_V} (\operatorname{div}(\tau_h^V), \boldsymbol{u}_h^V)_T \\ &- \sum_{F \in \mathcal{F}_V} ([\![(\tau_h^V)_{nn}]\!], (\boldsymbol{u}_h^V)_n)_F + ([\![(\tau_h^V)_{nt}]\!], \hat{\boldsymbol{u}}_h^V)_F,\end{aligned}$$

and the local residuum for the solution $\bar{\boldsymbol{u}}_h, \bar{p}_h$ of (8) with $\bar{\sigma}_h = \nu \nabla \bar{\boldsymbol{u}}_h$ given by

$$\begin{aligned}\boldsymbol{r}^V((\boldsymbol{v}_h^V, \hat{\boldsymbol{v}}_h^V)) := &\sum_{T \in \mathcal{T}_V} (\boldsymbol{f}, \boldsymbol{B}^V(\boldsymbol{v}_h^V))_T + \sum_{T \in \mathcal{T}_V} (\nu \Delta \bar{\boldsymbol{u}}_h - \nabla \bar{p}_h, \boldsymbol{B}^V(\boldsymbol{v}_h^V))_T \\ &- ((\bar{\sigma}_h - \bar{p}_h I_{d\times d})_{nn}, (\boldsymbol{B}^V(\boldsymbol{v}_h^V))_n)_{\partial T} - (\phi_V(\bar{\sigma}_h)_{nt}, \hat{\boldsymbol{v}}_h^V)_{\partial T}.\end{aligned}$$

Note that $\langle \operatorname{div}(\cdot), (\cdot,\cdot)\rangle_{\boldsymbol{V}_h^V}$ reads as a restriction of the discrete duality pair $\langle \operatorname{div}(\cdot), \cdot\rangle_{\boldsymbol{V}_h}$ onto ω_V but further includes the normal-tangential jumps since functions in Σ_h^V are not (normal-tangential) continuous. This shows that (31) reads as a local version of the global problem given by (27) where the (normal-tangential) continuity of the stress variable σ_h^V is incorporated by a Lagrange multiplier in $\hat{\boldsymbol{V}}_h^V$.

Using integration by parts, the right hand side can also be written as

$$\begin{aligned}\boldsymbol{r}^V((\boldsymbol{v}_h^V, \hat{\boldsymbol{v}}_h^V)) = &\sum_{T \in \mathcal{T}_V} (\boldsymbol{f}, \boldsymbol{B}^V(\boldsymbol{v}_h^V))_T - (\bar{\sigma}_h, \nabla \boldsymbol{B}^V(\boldsymbol{v}_h^V))_T \\ &+ (\bar{p}_h, \operatorname{div}(\boldsymbol{B}^V(\boldsymbol{v}_h^V)))_T + ((\bar{\sigma}_h)_{nt}, (\boldsymbol{B}^V(\boldsymbol{v}_h^V) - \phi_V \hat{\boldsymbol{v}}_h^V)_t)_{\partial T}.\end{aligned} \tag{33}$$

Remark 7.2. As usual for equilibrated error estimators we slightly modify the definition of the local problems when the vertex V lies on the Dirichlet boundary. In this case the degrees of freedom of $\hat{\boldsymbol{V}}_h^V$ on the domain boundary are removed. Accordingly, $\mathcal{F}_V$ gets replaced by $\mathcal{F}_V \setminus \{F \in \mathcal{F}_V : F \subset \partial\Omega\}$. Moreover, the mean value constraint of the product space is removed, i.e. we set $\boldsymbol{X}_h^V := (\boldsymbol{V}_h^V \times \hat{\boldsymbol{V}}_h^V)$.

7.2. **Analysis of the local problem.** For the analysis consider the norms

$$\|\sigma_h^V\|_{\Sigma_h^V}^2 := \sum_T \|\sigma_h^V\|_T^2 + h_T\|(\sigma_h^V)_{nt}\|_{\partial T}^2,$$
$$\|(\boldsymbol{v}_h^V, \hat{\boldsymbol{v}}_h^V)\|_{\boldsymbol{X}_h^V}^2 := \sum_T \|\nabla \boldsymbol{v}_h^V\|_T^2 + \frac{1}{h_T}\|(\hat{\boldsymbol{v}}_h^V - \boldsymbol{v}_h^V)_t\|_{\partial T}^2,$$
$$\|p_h^V\|_{Q_h^V} = \|p_h^V\|_{\omega_V}.$$

Note that the the norm $\|\cdot\|_{\boldsymbol{X}_h^V}$ reads as an H^1-like norm on the velocity space $\boldsymbol{X}_h$ since the Lagrange multipliers in $\hat{\boldsymbol{V}}_h^V$ can be interpreted as the tangential component of the local velocities in $\boldsymbol{V}_h^V$. Such norms are very common in the analysis of hybrid discontinuous Galerkin methods, see for example [25]. Further we define the kernel of the constraints given by

$$\mathcal{K}^V := \{(\sigma_h^V, p_h^V) \in \Sigma_h^V \times Q_h^V : \forall (\boldsymbol{v}_h^V, \hat{\boldsymbol{v}}_h^V) \in \boldsymbol{X}_h^V, \\ \langle \mathrm{div}(\sigma_h^V), (\boldsymbol{v}_h^V, \hat{\boldsymbol{v}}_h^V)\rangle_{\boldsymbol{V}_h^V} + (\mathrm{div}(\boldsymbol{v}_h^V), p_h^V)_{\omega_V} = 0\}.$$

Lemma 7.3. The following stability conditions hold true:

- Continuity: For all $\sigma_h^V, \tau_h^V \in \Sigma_h^V$, $(\boldsymbol{v}_h^V, \hat{\boldsymbol{v}}_h^V) \in \boldsymbol{X}_h^V$ and $q_h \in Q_h^V$ we have
$$(\sigma_h^V, \tau_h^V)_{\omega_V} \lesssim \|\sigma_h^V\|_{\Sigma_h^V}\|\tau^V\|_{\Sigma_h^V},$$
$$\langle \mathrm{div}(\sigma_h^V), (\boldsymbol{v}_h^V, \hat{\boldsymbol{v}}_h^V)\rangle_{\boldsymbol{V}_h^V} \lesssim \|\sigma_h^V\|_{\Sigma_h^V}\|(\boldsymbol{v}_h^V, \hat{\boldsymbol{v}}_h^V)\|_{\boldsymbol{X}_h^V},$$
$$(\mathrm{div}(\boldsymbol{v}_h^V), q_h^V)_{\omega_V} \lesssim \|(\boldsymbol{v}_h^V, \hat{\boldsymbol{v}}_h^V)\|_{\boldsymbol{X}_h^V}\|q_h\|_{Q_h^V}.$$
- Kernel coercivity: For all $(\sigma_h^V, p_h^V) \in \mathcal{K}^V$ we have
$$(\sigma_h^V, \tau_h^V)_{\omega_V} \gtrsim (\|\sigma_h^V\|_{\Sigma_h^V}^2 + \|p_h^V\|_{Q_h^V}^2).$$
- The inf-sup conditions:
  i. For all $(\boldsymbol{v}_h^V, \hat{\boldsymbol{v}}_h^V) \in \boldsymbol{X}_h^V$ there exists a constant $\beta_1 > 0$ such that
$$\sup_{(\sigma_h^V, p_h^V) \in \Sigma_h^V \times Q_h^V} \frac{\langle \mathrm{div}(\sigma_h^V), (\boldsymbol{v}_h^V, \hat{\boldsymbol{v}}_h^V)\rangle_{\boldsymbol{V}_h^V} + (\mathrm{div}(\boldsymbol{v}_h^V), p_h^V)_{\omega_V}}{\|\sigma_h^V\|_{\Sigma_h^V}\| + \|p_h^V\|_{Q_h^V}} \geq \beta_1 \|(\boldsymbol{v}_h^V, \hat{\boldsymbol{v}}_h^V)\|_{\boldsymbol{X}_h^V}.$$
  ii. For all $(\boldsymbol{v}_h^V, \hat{\boldsymbol{v}}_h^V) \in \boldsymbol{X}_h^V$ with $\mathrm{div}(\boldsymbol{v}_h^V) = 0$ there exists a constant $\beta_2 > 0$ such that
$$\sup_{\sigma_h^V \in \Sigma_h^V} \frac{\langle \mathrm{div}(\sigma_h^V), (\boldsymbol{v}_h^V, \hat{\boldsymbol{v}}_h^V)\rangle_{\boldsymbol{V}_h^V}}{\|\sigma_h^V\|_{\Sigma_h^V}} \geq \beta_2 \|(\boldsymbol{v}_h^V, \hat{\boldsymbol{v}}_h^V)\|_{\boldsymbol{X}_h^V}.$$

Proof. The continuity follows immediately with the Cauchy–Schwarz inequality and using integration by parts for integrals of the bilinear form $\langle \mathrm{div}(\cdot), (\cdot,\cdot)\rangle_{\boldsymbol{V}_h^V}$. The proofs of the kernel ellipticity and the inf-sup conditions follow with exactly the same steps as in the stability proofs of the original MCS-method in [18, 17, 24], since the bilinear forms and spaces of the local problems in this work simply read as a hybridized version of the original MCS-method. In this work the normal-tangential continuity of the stress space is incorporated by the additional Lagrange multiplier $\hat{\boldsymbol{u}}_h^V$ and we switched from the H^1-like DG norm used in the original works to the corresponding H^1-like HDG norm given by $\|\cdot\|_{\boldsymbol{X}_h^V}$ in this work. Note however, that we do not have zero Dirichlet boundary conditions of the velocity variable, but since we excluded the kernel of $\|\cdot\|_{\boldsymbol{X}_h^V}$ (constant functions) in the definition of the space $\boldsymbol{X}_h^V$, the results simply follow by norm equivalence. □

Theorem 7.4. There exists a unique solution $(\sigma_h^V, (\boldsymbol{u}_h^V, \hat{\boldsymbol{u}}_h^V), p_h^V) \in \Sigma_h^V \times \boldsymbol{X}_h^V \times Q_h^V$ of (31) with the stability estimate

$$\|\sigma_h^V\|_{\Sigma_h^V} + \|(\boldsymbol{u}_h^V, \hat{\boldsymbol{u}}_h^V)\|_{\boldsymbol{X}_h^V} \lesssim \sup_{\substack{(\boldsymbol{v}_h^V, \hat{\boldsymbol{v}}_h^V) \in \boldsymbol{X}_h^V \\ \mathrm{div}(\boldsymbol{v}_h^V) = 0}} \frac{\boldsymbol{r}^V((\boldsymbol{v}_h^V, \hat{\boldsymbol{v}}_h^V))}{\|(\boldsymbol{v}_h^V, \hat{\boldsymbol{v}}_h^V)\|_{\boldsymbol{X}_h^V}}$$

Proof. The solvability of (31) follows with the standard theory of saddle point problems (i.e. Brezzi's Theorem), see for example in [4] and the estimitates of Lemma 7.3. The stability estimate follows by the inf-sup condition on the subspace of divergence-free functions, see item ii. of Lemma 7.3, and standard estimates employing the solvability of (31). □

Now let $\hat{\boldsymbol{V}}_h$ be the global version of the local space $\hat{\boldsymbol{V}}_h^V$, i.e. we define

$$\hat{\boldsymbol{V}}_h := \{\hat{\boldsymbol{v}}_h \in \boldsymbol{L}^2(\mathcal{F}) : \forall F \in \mathcal{F},\ \hat{\boldsymbol{v}}_h|_F \in \boldsymbol{P}_k(F) \text{ and } (\hat{\boldsymbol{v}}_h)_n = 0\}.$$

The next theorem provides several properties of the local solution of (31). First we show that equation (31b) also holds for constants (and not only for functions of the factor space $\boldsymbol{X}_h^V$), and that the local stress variable has a vanishing normal-tangential trace. Further we discuss local equilibrium conditions.

Theorem 7.5 (Properties of the local solution)**.** Let $\sigma_h^V \in \Sigma_h^V$ and $p_h^V \in Q_h^V$ be the local solution of (31). There hold the following properties:

i. For all $(\boldsymbol{v}_h^V, \hat{\boldsymbol{v}}_h^V) \in \boldsymbol{V}_h^V \times \hat{\boldsymbol{V}}_h^V$ there holds

$$\langle \operatorname{div}(\sigma_h^V), (\boldsymbol{v}_h^V, \hat{\boldsymbol{v}}_h^V)\rangle_{\boldsymbol{V}_h^V} + (\operatorname{div}(\boldsymbol{v}_h^V), p_h^V)_{\omega_V} = \boldsymbol{r}^V((\boldsymbol{v}_h^V, \hat{\boldsymbol{v}}_h^V)). \tag{34}$$

ii. For any $(\boldsymbol{v}_h, \hat{\boldsymbol{v}}_h)$ of the (global) space $\boldsymbol{V}_h \times \hat{\boldsymbol{V}}_h$, with $\operatorname{div}(\boldsymbol{v}_h) = 0$, there holds the local equilibrium condition

$$\langle \operatorname{div}(\sigma_h^V), (\boldsymbol{v}_h, \hat{\boldsymbol{v}}_h)\rangle_{\boldsymbol{V}_h^V} = \boldsymbol{r}^V((\boldsymbol{v}_h, \hat{\boldsymbol{v}}_h)). \tag{35}$$

iii. The solution σ_h^V has a zero normal-tangential trace at the boundary

$$(\sigma_h^V)_{nt} = 0 \quad \text{on} \quad \partial\omega_V.$$

Proof. Let $V \in \mathcal{V}$ be an arbitrary but fixed vertex. In a first step we will proof that equation (31b) also hold for constant functions. To this end let $\boldsymbol{c} = \boldsymbol{\pi}_{\mathbb{R}}^V((\boldsymbol{v}_h^V, \hat{\boldsymbol{v}}_h^V))$. Using $\operatorname{div}(\boldsymbol{c}) = 0$ and integration by parts we have for the left side of (31b)

$$\begin{aligned}
\langle \operatorname{div}(\sigma_h^V), (\boldsymbol{c}, \boldsymbol{c}_t)\rangle_{\boldsymbol{V}_h^V} &+ (\operatorname{div}(\boldsymbol{c}), p_h^V)_{\omega_V} \\
&= \sum_T (\operatorname{div}(\sigma_h^V), \boldsymbol{c})_T - \sum_F ([\![(\sigma_h^V)_{nn}]\!], \boldsymbol{c}_n)_F + ([\![(\sigma_h^V)_{nt}]\!], \boldsymbol{c}_t)_F \\
&= -\sum_T (\sigma_h^V, \nabla \boldsymbol{c})_T + \sum_F ([\![(\sigma_h^V)_{nt}]\!], (\boldsymbol{c} - \boldsymbol{c})_t)_F = 0.
\end{aligned}$$

We continue with the right-hand side. Using representation (33) we get for the constant $\boldsymbol{c}$ and using item iv. of Lemma 7.1 that

$$\begin{aligned}
\boldsymbol{r}^V((\boldsymbol{c}, \boldsymbol{c}_t)) &= \sum_{T\in\mathcal{T}_V} (\boldsymbol{f}, \boldsymbol{B}^V(\boldsymbol{c}))_T - (\bar{\sigma}_h, \nabla \boldsymbol{B}^V(\boldsymbol{c}))_T + (\phi_V \bar{p}_h, \operatorname{div}(\boldsymbol{B}^V(\boldsymbol{c})))_T \\
&\quad + ((\bar{\sigma}_h)_{nt}, (\boldsymbol{B}^V(\boldsymbol{c})_t - \phi_V \boldsymbol{c}_t))_{\partial T} \\
&= \sum_{T\in\mathcal{T}_V} (\boldsymbol{f}, \boldsymbol{c}\phi_V)_T - (\bar{\sigma}_h, \nabla(\boldsymbol{c}\phi_V))_T + (\bar{p}_h \operatorname{div}(\boldsymbol{c}\phi_V))_T.
\end{aligned}$$

Since $\boldsymbol{c}\phi_V$ is an element of the velocity Stokes discretisation space $\bar{\boldsymbol{V}}_h$, the first line of (8) then gives

$$\boldsymbol{r}^V((\boldsymbol{c}, \boldsymbol{c}_t)) = \sum_{T\in\mathcal{T}_V} (\boldsymbol{f}, (\mathbf{id} - \mathcal{R})\boldsymbol{c}\phi_V)_T = 0,$$

where the last step follows from $\boldsymbol{c}\phi_V \in \boldsymbol{P}_1(\mathcal{T}) \cap \boldsymbol{H}_0^1(\Omega)$ and (10). In total this shows that we also have $\boldsymbol{r}^V((\boldsymbol{c}, \boldsymbol{c}_t)) = 0$, thus using $(\boldsymbol{v}_h^V, \hat{\boldsymbol{v}}_h^V) = (\boldsymbol{\pi}_{\mathbb{R}}^V + (\mathbf{id} - \boldsymbol{\pi}_{\mathbb{R}}^V))(\boldsymbol{v}_h^V, \hat{\boldsymbol{v}}_h^V)$, definition (30) and (31b), we have proven (34).

For the second statement let $(\boldsymbol{v}_h, \hat{\boldsymbol{v}}_h) \in \boldsymbol{V}_h \times \hat{\boldsymbol{V}}_h$, with $\operatorname{div}(\boldsymbol{v}_h) = 0$. Setting $\boldsymbol{v}_h^V = \boldsymbol{v}_h|_{\omega_V}$ and $\hat{\boldsymbol{v}}_h^V = \hat{\boldsymbol{v}}_h|_{\mathcal{F}_V}$ immediately proves (35).

For the proof of the third statement consider the test function $\hat{\boldsymbol{v}}_h^V \in \hat{\boldsymbol{V}}_h^V$ such that $\hat{\boldsymbol{v}}_h^V = (\sigma_h^V)_{nt}$ on every facet $F \subset \partial\omega_V$, and zero on the internal facets. Using equation (34) with $\boldsymbol{v}_h^V = 0$ then gives (for the squared L^2-norm on the facets)

$$\sum_{F\in\partial\omega_V} ((\sigma_h^V)_{nt}, (\sigma_h^V)_{nt})_F = \sum_{F\in\partial\omega_V} ((\sigma_h^V)_{nt}, \hat{\boldsymbol{v}}_h^V)_F = \sum_{T\in\mathcal{T}_V} (\phi_V(\bar{\sigma}_h)_{nt}, \hat{\boldsymbol{v}}_h^V)_{\partial T} = 0,$$

where we used that ϕ_V vanishes on the boundary $\partial\omega_V$ and $\hat{\boldsymbol{v}}_h^V$ on internal facets. □

7.3. **Admissibility of the global flux.** After solving the local problems we define the equilibrated flux

$$\sigma_h^{\mathsf{LEQ}} := \bar{\sigma}_h - \sigma_h^{\Delta} \quad \text{with} \quad \sigma_h^{\Delta} := \sum_V \sigma_h^V. \tag{36}$$

Theorem 7.6. The locally equilibrated stress σ_h^{LEQ} is an element of Σ_h and satisfies the discrete equilibration condition (24), i.e.,

$$(\boldsymbol{f}, \boldsymbol{v}_h) + \langle \mathrm{div}(\sigma_h^{\mathsf{LEQ}}), \boldsymbol{v}_h\rangle_{\boldsymbol{V}_h} = 0 \quad \text{for all } \boldsymbol{v}_h \in \boldsymbol{V}_h \text{ with } \mathrm{div}(\boldsymbol{v}_h) = 0.$$

Proof. To show $\sigma_h^{\mathsf{LEQ}} \in \Sigma_h$ it suffices to show that its normal-tangential jumps vanish. Indeed, for any arbitrary $\hat{\boldsymbol{v}}_h \in \hat{\boldsymbol{V}}_h$, it holds,

$$\begin{aligned}\sum_{F\in\mathcal{F}} ([\![(\sigma_h^{\mathsf{LEQ}})_{nt}]\!], (\hat{\boldsymbol{v}}_h)_t)_F &= \sum_{V\in\mathcal{V}}\sum_{F\in\mathcal{F}_V} ([\![(\sigma_h^{\mathsf{LEQ}})_{nt}]\!], (\phi_V\hat{\boldsymbol{v}}_h)_t)_F \\ &= \sum_{V\in\mathcal{V}}\sum_{F\in\mathcal{F}_V} ([\![(\bar{\sigma}_h)_{nt}]\!], (\phi_V\hat{\boldsymbol{v}}_h)_t)_F - ([\![(\sigma_h^{\Delta})_{nt}]\!], (\phi_V\hat{\boldsymbol{v}}_h)_t)_F.\end{aligned}$$

Here, we only used that the $\{\phi_V\}_{V\in\mathcal{V}}$ form a partition of unity. Applying the third and then the second statement of Theorem 7.5 (with $\boldsymbol{v}_h = 0$), the sum over the last integral can be written as

$$\begin{aligned}\sum_{V\in\mathcal{V}}\sum_{F\in\mathcal{F}_V} ([\![(\sigma_h^{\Delta})_{nt}]\!], (\phi_V\hat{\boldsymbol{v}}_h)_t)_F &= \sum_{V\in\mathcal{V}}\sum_{F\in\mathcal{F}_V} ([\![(\sigma_h^{V})_{nt}]\!], (\phi_V\hat{\boldsymbol{v}}_h)_t)_F \\ &= \sum_{V\in\mathcal{V}}\sum_{F\in\mathcal{F}_V} ([\![(\bar{\sigma}_h)_{nt}]\!], (\phi_V\hat{\boldsymbol{v}}_h)_t)_F,\end{aligned}$$

and thus $\sum_{F\in\mathcal{F}}([\![(\sigma_h^{\mathsf{LEQ}})_{nt}]\!], (\hat{\boldsymbol{v}}_h)_t)_F = 0$. With the choice $(\hat{\boldsymbol{v}}_h)_t = [\![(\sigma_h^{\mathsf{LEQ}})_{nt}]\!]$, we conclude that $[\![(\sigma_h^{\mathsf{LEQ}})_{nt}]\!] = 0$ point wise, and so $\sigma_h^{\mathsf{LEQ}} \in \Sigma_h$.

To show the equilibration constraint, consider an arbitrary $\boldsymbol{v}_h \in \boldsymbol{V}_h$ with $\mathrm{div}(\boldsymbol{v}_h) = 0$. Since $\sigma_h^{\mathsf{LEQ}} \in \Sigma_h$, the definition of the global and local distributional divergences and (36) gives

$$\begin{aligned}\langle \mathrm{div}(\sigma_h^{\mathsf{LEQ}}), \boldsymbol{v}_h\rangle_{\boldsymbol{V}_h} &= \langle \mathrm{div}(\bar{\sigma}_h), \boldsymbol{v}_h\rangle_{\boldsymbol{V}_h} - \sum_{V\in\mathcal{V}} \langle \mathrm{div}(\sigma_h^V), (\boldsymbol{v}_h, \boldsymbol{0})\rangle_{\boldsymbol{V}_h^V} \\ &= \langle \mathrm{div}(\bar{\sigma}_h), \boldsymbol{v}_h\rangle_{\boldsymbol{V}_h} - \sum_{V\in\mathcal{V}} \boldsymbol{r}^V((\boldsymbol{v}_h, \boldsymbol{0})) = -(\boldsymbol{f}, \boldsymbol{v}_h).\end{aligned}$$

The last identity follows with an integration by parts, item iii. of Lemma 7.1 and $\mathrm{div}(\boldsymbol{v}_h) = 0$. Altogether this shows the claimed discrete equilibration condition. □

8. Local Efficiency

This section proves efficiency of the proposed local equilibrated fluxes in the sense that the error estimator is a lower bound for the velocity error plus norms that only depend on the velocity and have the right order and data oscillations. In particular also the efficiency bound is pressure-independent.

Theorem 8.1 (Efficiency of the local design)**.** Assume that the exact solution fulfills the regularity $\boldsymbol{u} \in \boldsymbol{H}^m(\mathcal{T}) \cap V_0$, for some $m \geq 2$. The error estimator for $\sigma_h := \sigma_h^{\mathsf{LEQ}}$ is efficient in the sense that

$$\eta(\sigma_h^{\mathsf{LEQ}}) \lesssim \nu^{-1}\Big(\|\sigma - \bar{\sigma}_h\| + \sum_{V\in\mathcal{V}} \|\sigma_h^V\|_{\Sigma_h^V} + \operatorname{osc}_{k-2}(\operatorname{curl}(\boldsymbol{f}))\Big),$$

where $\sigma_h^V \in \Sigma_h^V$ are the local solutions of (31) and the oscillations as in Theorem 6.2. Further there holds for all local solutions the pressure-robust local efficiency

$$\|\sigma_h^V\|_{\Sigma_h^V}^2 \lesssim \sum_{T\in\mathcal{T}_V} \|\sigma - \bar{\sigma}_h\|_T^2 + h_T\|(\sigma - \bar{\sigma}_h)_{nt}\|_{\partial T}^2 + h_T^2\|(\mathbf{id} - \boldsymbol{\pi}_{r-2})\nu\Delta\boldsymbol{u}\|_T^2.$$

If the reconstruction operator $\mathcal{R}$ of the primal method (8) is the identity, the last term of the right hand side vanishes.

Proof. The first statement follows with exactly the same steps as in the proof Theorem 6.2, equation (36) and the triangle inequality

$$\|\sigma - \sigma_h^{\mathsf{LEQ}}\| \leq \|\sigma - \bar{\sigma}_h\| + \|\sum_{V\in\mathcal{V}} \sigma_h^V\| \leq \|\sigma - \bar{\sigma}_h\| + \sum_{V\in\mathcal{V}} \|\sigma_h^V\|_{\Sigma_h^V}.$$

We continue with the proof of the local pressure-robust stability estimate. For this let $(\sigma_h^V, (\boldsymbol{u}_h^V, \hat{\boldsymbol{u}}_h^V), p_h^V) \in \Sigma_h^V \times \boldsymbol{X}_h^V \times Q_h^V$ be the solution of (31). By the stability estimate of Theorem 7.4 we have

$$\|\sigma_h^V\|_{\Sigma_h^V} \lesssim \sup_{\substack{(\boldsymbol{v}_h^V, \hat{\boldsymbol{v}}_h^V)\in\boldsymbol{X}_h^V \\ \operatorname{div}(\boldsymbol{v}_h^V)=0}} \frac{\boldsymbol{r}^V((\boldsymbol{v}_h^V, \hat{\boldsymbol{v}}_h^V))}{\|(\boldsymbol{v}_h^V, \hat{\boldsymbol{v}}_h^V)\|_{\boldsymbol{X}_h^V}}.$$

Let $(\boldsymbol{v}_h^V, \hat{\boldsymbol{v}}_h^V) \in \boldsymbol{X}_h^V$ with $\operatorname{div}(\boldsymbol{v}_h) = 0$ be arbitrary. With $\boldsymbol{f} = -\Delta\boldsymbol{u} + \nabla p$ and applying integration by parts (similar to (33)), the numerator simplifies to

$$\boldsymbol{r}^V((\boldsymbol{v}_h^V, \hat{\boldsymbol{v}}_h^V)) = \sum_{T\in\mathcal{T}_V} (\sigma - \bar{\sigma}_h, \nabla\boldsymbol{B}^V(\boldsymbol{v}_h^V))_T \tag{37}$$

$$- \sum_{T\in\mathcal{T}_V} ((\sigma - \bar{\sigma}_h)_{nt}, (\boldsymbol{B}^V(\boldsymbol{v}_h^V) - \phi_V\hat{\boldsymbol{v}}_h^V)_t)_{\partial T} \tag{38}$$

$$- \sum_{T\in\mathcal{T}_V} (p - \bar{p}_h, \operatorname{div}(\boldsymbol{B}^V(\boldsymbol{v}_h^V)))_T, \tag{39}$$

where we used that $\boldsymbol{B}^V(\boldsymbol{v}_h^V)\cdot\boldsymbol{n} = 0$ on $\partial\omega_V$ (see item i. of Lemma 7.1) and that

$$\sum_{T\in\mathcal{T}_V} (\phi_V(\sigma)_{nt}, (\hat{\boldsymbol{v}}_h^V)_t)_{\partial T} = \sum_{F\in\mathcal{F}_V} ([\![\phi_V(\sigma)_{nt}]\!], (\hat{\boldsymbol{v}}_h^V)_t)_F = 0.$$

By the continuity of the bubble projector $\boldsymbol{B}^V$ and that $\phi_V = \mathcal{O}(1)$ on ω_V, the Cauchy–Schwarz inequality applied to the sums in (37) and (38) gives

$$\begin{aligned}
&\sum_{T\in\mathcal{T}_V} (\sigma - \bar{\sigma}_h, \nabla\boldsymbol{B}^V(\boldsymbol{v}_h^V))_T - ((\sigma - \bar{\sigma}_h)_{nt}, (\boldsymbol{B}^V(\boldsymbol{v}_h^V) - \phi_V\hat{\boldsymbol{v}}_h^V)_t)_{\partial T} \\
&\leq \sum_{T\in\mathcal{T}_V} \|(\sigma - \bar{\sigma}_h)\|_T\|\nabla\boldsymbol{v}_h^V\|_T + h_T\|(\sigma - \bar{\sigma}_h)_{nt}\|_{\partial T}\frac{1}{h_T}\|(\boldsymbol{v}_h^V - \hat{\boldsymbol{v}}_h^V)_t\|_{\partial T} \\
&\leq \left(\sum_{T\in\mathcal{T}_V} \|(\sigma - \bar{\sigma}_h)\|_T^2 + h_T^2\|(\sigma - \bar{\sigma}_h)_{nt}\|_{\partial T}^2\right)^{1/2} \|(\boldsymbol{v}_h^V, \hat{\boldsymbol{v}}_h^V)\|_{\boldsymbol{X}_h^V}.
\end{aligned}$$

We continue with the remaining third sum in (39) (which does not vanish, although $\boldsymbol{v}_h^V$ is divergence-free). For this let $\pi^{\bar{Q}_h}p$ be the L^2 best-approximation of the exact pressure in the pressure space $\bar{Q}_h$ and define the mean

value

$$c_p := \frac{1}{|\mathcal{T}_V|}(\pi^{\bar{Q}_h} p - \bar{p}_h, 1)_{\omega_V}.$$

According to item ii. of Lemma 7.1, we have that $\boldsymbol{B}^V(\boldsymbol{v}_h^V) \in \mathrm{BDM}_k(\mathcal{T}_V)$ and thus $\mathrm{div}(\boldsymbol{B}^V(\boldsymbol{v}_h^V)) \in \bar{Q}_h$, which gives

$$\begin{aligned}\sum_{T\in\mathcal{T}_V} (p - \bar{p}_h, \mathrm{div}(\boldsymbol{B}^V(\boldsymbol{v}_h^V)))_T &= \sum_{T\in\mathcal{T}_V} (\pi^{\bar{Q}_h} p - \bar{p}_h - c_p, \mathrm{div}(\boldsymbol{B}^V(\boldsymbol{v}_h^V)))_T \\ &\lesssim \|\pi^{\bar{Q}_h} p - \bar{p}_h - c_p\|_{\omega_V} \|(\boldsymbol{v}_h^V, \hat{\boldsymbol{v}}_h^V)\|_{\boldsymbol{X}_h^V},\end{aligned}$$

where we again used the continuity of $\boldsymbol{B}^V$. By the inf-sup condition of the primal Stokes dicretisation ($\pi^{\bar{Q}_h} p - \bar{p}_h - c_p$ has a zero mean value on ω_V) on the local space $\bar{\boldsymbol{V}}_h \cap H_0^1(\omega_V)$ we have

$$\|\pi^{\bar{Q}_h} p - \bar{p}_h - c_p\|_{\omega_V} \lesssim \sup_{\bar{\boldsymbol{v}}_h \in \bar{\boldsymbol{V}}_h \cap H_0^1(\omega_V)} \frac{(\pi^{\bar{Q}_h} p - \bar{p}_h - c_p, \mathrm{div}(\bar{\boldsymbol{v}}_h))_{\omega_V}}{\|\nabla \bar{\boldsymbol{v}}_h\|_{\omega_V}}.$$

Now, using that $\bar{p}_h$ is the discrete pressure solution we get

$$\begin{aligned}-(\bar{p}_h, \mathrm{div}(\bar{\boldsymbol{v}}_h))_{\omega_V} &= (\boldsymbol{f}, \mathcal{R}(\bar{\boldsymbol{v}}_h))_{\omega_V} - (\nu \nabla \bar{\boldsymbol{u}}_h, \nabla \bar{\boldsymbol{v}}_h)_{\omega_V} \\ &= (-\nu\Delta \boldsymbol{u} + \nabla p, \mathcal{R}(\bar{\boldsymbol{v}}_h))_{\omega_V} - (\nu \nabla \bar{\boldsymbol{u}}_h, \nabla \bar{\boldsymbol{v}}_h)_{\omega_V}.\end{aligned}$$

Since $\mathrm{div}(\mathcal{R}(\bar{\boldsymbol{v}}_h)) \in \bar{Q}_h$, see (9a), we get using integration by parts

$$\begin{aligned}(\nabla p, \mathcal{R}(\bar{\boldsymbol{v}}_h))_{\omega_V} = -(p, \mathrm{div}(\mathcal{R}(\bar{\boldsymbol{v}}_h)))_{\omega_V} &= -(\pi^{\bar{Q}_h} p, \mathrm{div}(\mathcal{R}(\bar{\boldsymbol{v}}_h)))_{\omega_V} \\ &= -(\pi^{\bar{Q}_h} p, \mathrm{div}(\bar{\boldsymbol{v}}_h))_{\omega_V},\end{aligned}$$

and so in total (since $(c_p, \mathrm{div}(\bar{\boldsymbol{v}}_h))_{\omega_V} = 0$ by Gauss's theorem)

$$\begin{aligned}(\pi^{\bar{Q}_h} p - \bar{p}_h - c_p, \mathrm{div}(\bar{\boldsymbol{v}}_h))_{\omega_V} &= -(\nu\Delta \boldsymbol{u}, \mathcal{R}(\bar{\boldsymbol{v}}_h))_{\omega_V} - (\bar{\sigma}_h, \nabla \bar{\boldsymbol{v}}_h)_{\omega_V} \\ &= -(\nu\Delta \boldsymbol{u}, \mathcal{R}(\bar{\boldsymbol{v}}_h) - \bar{\boldsymbol{v}}_h)_{\omega_V} + (\sigma - \bar{\sigma}_h, \nabla \bar{\boldsymbol{v}}_h)_{\omega_V},\end{aligned}$$

where we added and subtracted (including integration by parts) $(\sigma, \nabla \bar{\boldsymbol{v}}_h)_{\omega_V}$. By the properties of the reconstruction operator, the first integral can be bounded by

$$(-\nu\Delta \boldsymbol{u}, \mathcal{R}(\bar{\boldsymbol{v}}_h) - \bar{\boldsymbol{v}}_h)_{\omega_V} \lesssim \|(\mathbf{id} - \boldsymbol{\pi}_{\omega_V}^{r-2})\nu\Delta \boldsymbol{u}\|_{\omega_V} h_V \|\nabla \bar{\boldsymbol{v}}_h\|_{\omega_V}, \tag{40}$$

where h_V denotes the diameter of the vertex patch ω_V. Thus by the Cauchy Schwarz inequality we get the estimate

$$\|\pi^{\bar{Q}_h} p - \bar{p}_h - c_p\|_{\omega_V} \lesssim h_V \|(\mathbf{id} - \boldsymbol{\pi}_{\omega_V}^{r-2})\nu\Delta \boldsymbol{u}\|_{\omega_V} + \left(\sum_{T\in\mathcal{T}_V} \|(\sigma - \bar{\sigma}_h)\|_T^2\right)^{1/2},$$

and so

$$\begin{aligned}\boldsymbol{r}^V((\boldsymbol{v}_h^V, \hat{\boldsymbol{v}}_h^V)) \lesssim \left(\sum_{T\in\mathcal{T}_V} \|(\sigma - \bar{\sigma}_h)\|_T^2 + h_T^2 \|(\sigma - \bar{\sigma}_h)_{nt}\|_{\partial T}^2\right)^{1/2} &\|(\boldsymbol{v}_h^V, \hat{\boldsymbol{v}}_h^V)\|_{\boldsymbol{X}_h^V} \\ + h_V \|(\mathbf{id} - \boldsymbol{\pi}_{\omega_V}^{r-2})\nu\Delta \boldsymbol{u}\|_{\omega_V} &\|(\boldsymbol{v}_h^V, \hat{\boldsymbol{v}}_h^V)\|_{\boldsymbol{X}_h^V}.\end{aligned}$$

This concludes the proof for the general case. Now assume that $\mathcal{R} = \mathbf{id}$, then we see that the additional term in (40) vanishes which proves the stated result in the case where no reconstruction operator in the primal method (8) is included. □

9. Numerical Examples

This section confirms the theoretical results by some numerical examples. For the ease of representation we introduce the following notation. The pressure-robust estimator of Theorem 5.2 is denoted by η. Here, the flux σ_h either corresponds to the solution ${\sigma_h}^{\mathsf{GEQ}}$ of the global problem (27) or to the local equilibrated flux ${\sigma_h}^{\mathsf{LEQ}}$ given by equation (36). Further, we track the error estimator contributions

$$\begin{aligned}\eta_{\mathbf{f}}(\sigma_h) &:= \nu^{-1}\|h_T^2(\mathbf{id}-\pi_{k-2})\operatorname{curl}(\mathbf{f})\|,\\ \eta_{\sigma}(\sigma_h) &:= \nu^{-1}\|\operatorname{dev}(\sigma_h-\bar{\sigma}_h)\|,\\ \eta_{\mathrm{div}} &:= c_0^{-1}\|\operatorname{div}(\bar{\boldsymbol{u}}_h)\|.\end{aligned}$$

Recall that Table 1 shows the different inf-sup stable velocity pressure pairs that we consider for the primal formulation (8). The order $k = r$ corresponds to the order of the space $\boldsymbol{V}_h = \mathrm{RT}_k$, i.e. the order of the spaces used in the equilibration designs (27) and (36). The adaptive mesh refinement loop is defined as usual by

$$\mathrm{SOLVE} \to \mathrm{ESTIMATE} \to \mathrm{MARK} \to \mathrm{REFINE} \to \mathrm{SOLVE} \to \dots$$

and employs the local contributions to the error estimator as element-wise refinement indicators. In the marking step, an element $T \in \mathcal{T}$ is marked for refinement if $\eta(T) \geq \frac{1}{4}\max_{K\in\mathcal{T}}\eta(K)$. The refinement step refines all marked elements plus further elements in a closure step to guarantee a regular triangulation.

In the case of the Scott–Vogelius (SV) finite element approximation, the adaptive algorithm includes two meshes: the macro element mesh $\mathcal{T}$ given by a standard triangulation, and the corresponding barycentrically refined triangulation (guaranteeing inf-sup stability of the SV element) denoted by $\mathcal{T}_{\mathrm{bar}}(\mathcal{T})$. Again, an element $T \in \mathcal{T}$ is marked if (mean value of the elements included in one macro element)

$$\frac{1}{3}\sum_{\substack{T'\in\mathcal{T}_{\mathrm{bar}}\\ T'\cap T\neq\emptyset}}\mu(T') \geq \frac{1}{4}\max_{K\in\mathcal{T}_{\mathrm{bar}}}\eta(K).$$

The refinement of $\mathcal{T}$ is done as described before. The final mesh is then obtained by a global barycentric refinement step. Note that although the macro element meshes are nested, their barycentric refinements are in general not nested.

The implementation and numerical examples where performed with the finite element library NGSolve/Netgen [41, 40], see also www.ngsolve.org.

	ref. level	0	1	2	3	4
$\nu = 1$	$\widetilde{\sigma}_h = \widetilde{\sigma}_h^{\mathsf{CEQ}}$	2.62	2.43	2.29	2.20	2.15
$\nu = 1$	$\sigma_h = \sigma_h^{\mathsf{GEQ}}$	2.30	1.75	1.29	1.14	1.07
$\nu = 1$	$\sigma_h = \sigma_h^{\mathsf{LEQ}}$	3.08	2.48	2.01	1.81	1.70
$\nu = 10^{-4}$	$\widetilde{\sigma}_h = \widetilde{\sigma}_h^{\mathsf{CEQ}}$	9526.38	11 515.79	9660.55	9633.06	9750.08
$\nu = 10^{-4}$	$\sigma_h = \sigma_h^{\mathsf{GEQ}}$	2.30	1.75	1.29	1.14	1.07
$\nu = 10^{-4}$	$\sigma_h = \sigma_h^{\mathsf{LEQ}}$	3.08	2.48	2.01	1.81	1.70

Table 2. Efficiency indices in the Example from Section 9.1 on uniformly refined meshes and the SV element.

9.1. **Smooth example on unit square.** First, we revisit the smooth example from Section 4.2. Figure 2 presents the convergence history of the error of the discrete Stokes solution $\bar{\boldsymbol{u}}_h$ measured in the H^1-semi norm using the SV element with two different viscosities $\nu = 1$ (top) and $\nu = 10^{-4}$ (bottom) on uniformly refined meshes. The first important observation is that the error plot for the pressure-robust error estimator $\eta(\sigma_h^{\mathsf{GEQ}})$ looks exactly the same for $\nu = 1$ and $\nu = 10^{-4}$, while the classical estimator $\widetilde{\eta}(\widetilde{\sigma}_h^{\mathsf{CEQ}})$ is nowhere close to the exact error of the pressure-robust Scott–Vogelius solution for $\nu = 10^{-4}$ as already observed in Section 4.2. As expected, the error estimator scales with ν^{-1} and so does its efficiency index.

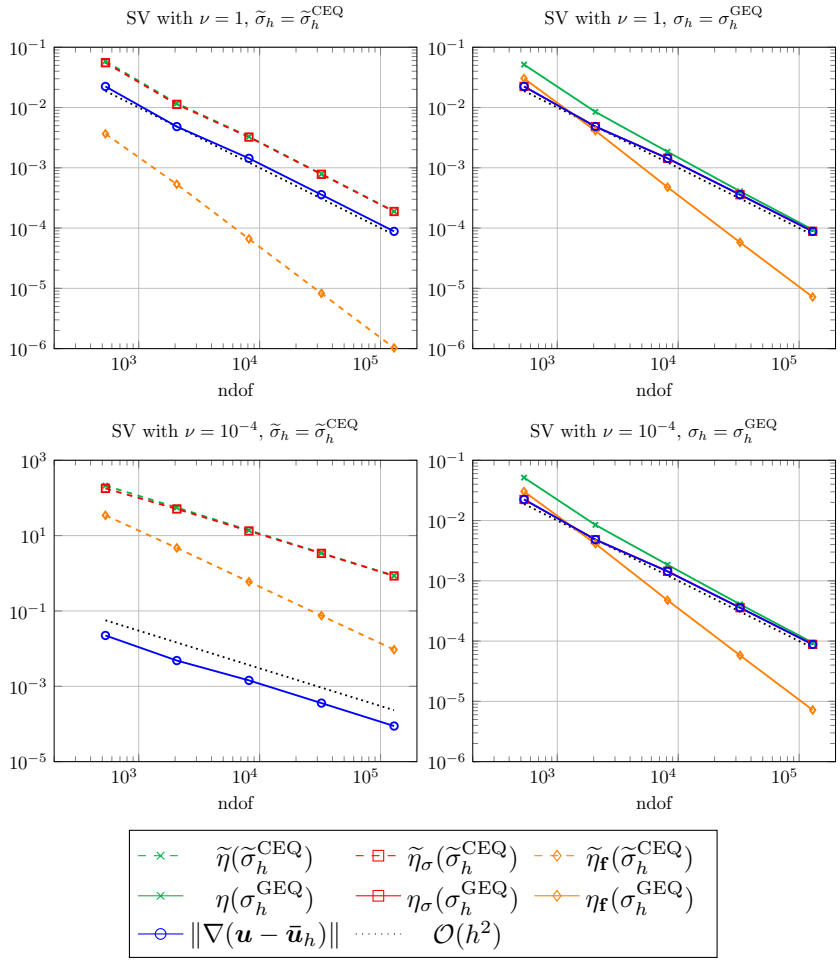

FIGURE 2. Example from Section 9.1: Convergence history of exact error and error estimator quantities on uniformly refined meshes for SV with $\nu = 1$ (top) and 10^{-4} (bottom) and $\sigma = \widetilde{\sigma}_h^{\mathrm{CEQ}}$ (left) and $\sigma = \sigma_h^{\mathrm{GEQ}}$ (right).

Table 2 lists the efficiency indices on the different refinement levels also for the pressure-robust local variant of our error estimator. One can see that the error estimator for $\eta(\sigma_h^{\mathrm{GEQ}})$ even is asymptotically exact, while the local variant is not, but still attains very good efficiency indices around 2. We want to mention again that the novel error bounds, unfortunately, contain unknown constants c_1 and c_2 which were evaluated by $c_1 = c_2 = 1$. However, they only appear in front of $\eta_{\boldsymbol{f}}$ which is a higher order term (see Figure 2 again).

9.2. **Smooth example on unit cube.** The second example extends the previous example onto the unit cube $\Omega = (0,1)^3$ by prescribing the solution

$$\boldsymbol{u}(x,y) := \operatorname{curl}(\xi,\xi,\xi) \quad \text{and} \quad p(x,y) := x^5 + y^5 + z^5 - 1/2$$

with the potential $\xi = x^2(1-x)^2y^2(1-y)^2z^2(1-z)^2$ and with matching right-hand side $\boldsymbol{f} := -\nu\Delta\boldsymbol{u} + \nabla p$ for variable viscosity ν.

Figure 3 presents the convergence history of the error of the discrete Stokes solution $\bar{\boldsymbol{u}}_h$ measured in the H^1-semi norm using the P2B-3d element with two different viscosities $\nu = 1$ (top) and $\nu = 10^{-4}$ (bottom) on uniformly refined meshes. The observations are similar to the ones in the two dimensional case which validates our results also for the case $d = 3$. Since the right-hand side $\boldsymbol{f}$ is a polynomial of higher order compared to the two dimensional example, the oscillation terms $\eta_{\boldsymbol{f}}({\sigma_h}^{\mathrm{GEQ}}), \widetilde{\eta}_{\boldsymbol{f}}(\widetilde{\sigma}_h^{\mathrm{CEQ}})$ are much larger and hence more dominating on coarser levels.

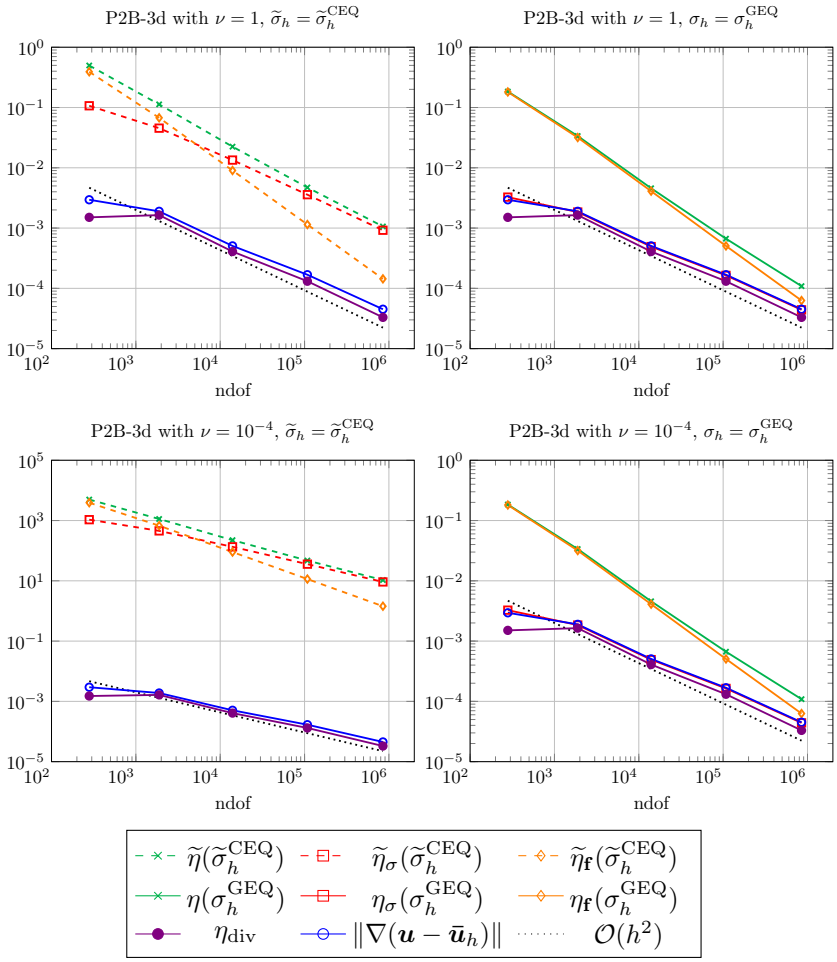

FIGURE 3. Example from Section 9.2: Convergence history of exact error and error estimator quantities on uniformly refined meshes for P2B-3d with $\nu = 1$ (top) and 10^{-4} (bottom) and $\sigma = \widetilde{\sigma}_h^{\mathrm{CEQ}}$ (left) and $\sigma = \sigma_h^{\mathrm{GEQ}}$ (right).

9.3. **L-shaped domain example.** The final example from [44] is defined on the L-shaped domain $\Omega := (-1,1)^2 \setminus \big((0,1) \times (-1,0)\big)$. The velocity $\boldsymbol{u}$ and pressure p_0 now satisfy $-\nu\Delta\boldsymbol{u} + \nabla p_0 = 0$, and read as (given in polar coordinates with radius R and angle φ)

$$\boldsymbol{u}(R,\varphi) := R^\alpha \begin{pmatrix} (\alpha+1)\sin(\varphi)\psi(\varphi) + \cos(\varphi)\psi'(\varphi) \\ -(\alpha+1)\cos(\varphi)\psi(\varphi) + \sin(\varphi)\psi'(\varphi) \end{pmatrix}^T,$$
$$p_0 := \nu R^{(\alpha-1)}((1+\alpha)^2\psi'(\varphi) + \psi'''(\varphi))/(1-\alpha)$$

with

$$\psi(\varphi) := 1/(\alpha+1)\,\sin((\alpha+1)\varphi)\cos(\alpha\omega) - \cos((\alpha+1)\varphi) \\ - 1/(\alpha-1)\,\sin((\alpha-1)\varphi)\cos(\alpha\omega) + \cos((\alpha-1)\varphi),$$

and $\alpha = 856399/1572864 \approx 0.54$, $\omega = 3\pi/2$. To have a nonzero right-hand side we add the pressure $p_+ := \sin(xy\pi)$, i.e. $p := p_0 + p_+$ and $\boldsymbol{f} := \nabla(p_+)$. Note that since $\boldsymbol{f}$ is a gradient we have $\eta_{\boldsymbol{f}} = 0$ in this example.

Figure 4 shows the convergence history of the exact error and the error estimators based on the classical equilibrated fluxes $\widetilde{\sigma}_h^{\mathrm{CEQ}}$ and the pressure-robust fluxes σ_h^{GEQ} on adaptively refined meshes where the refinement indicators are steered by the local contributions of the estimators. For $\nu = 1$ both estimators are efficient, the

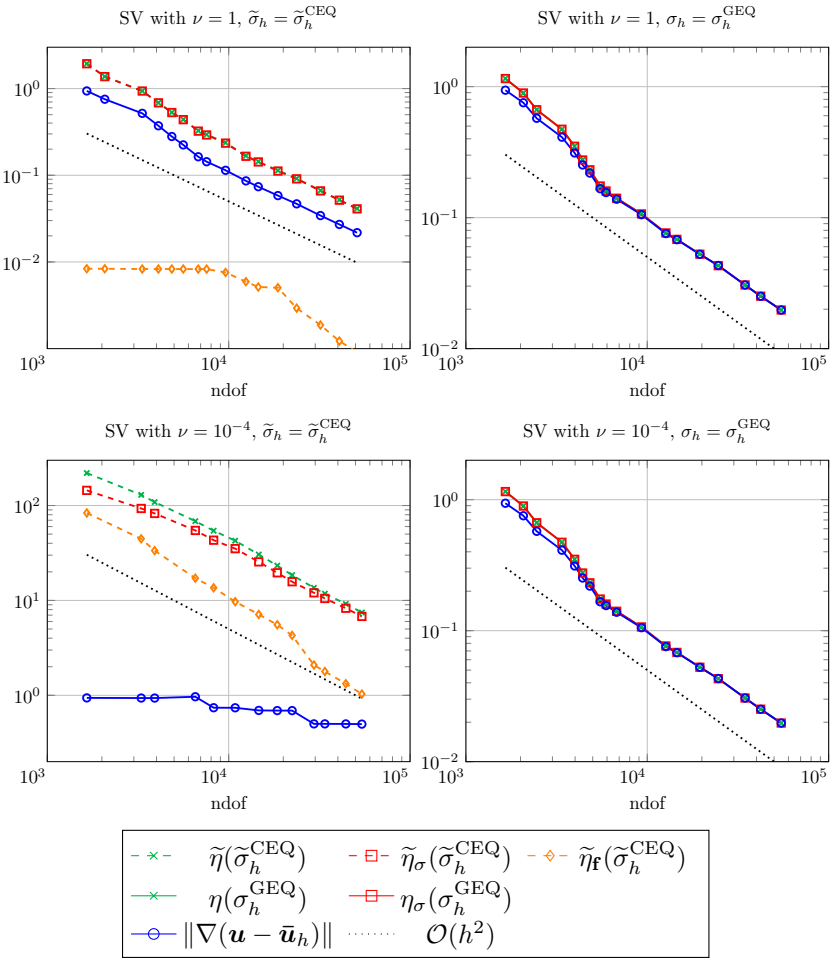

FIGURE 4. Example from Section 9.3: Convergence history of exact error and error estimator quantities on adaptively refined meshes for SV with $\nu = 1$ (top) and 10^{-4} (bottom) and $\sigma_h = \widetilde{\sigma}_h^{\mathrm{CEQ}}$ (left) and $\sigma_h = \sigma_h^{\mathrm{GEQ}}$ (right).

	ref. level	$\mathrm{ref}_{\mathrm{tot}} - 4$	$\mathrm{ref}_{\mathrm{tot}} - 3$	$\mathrm{ref}_{\mathrm{tot}} - 2$	$\mathrm{ref}_{\mathrm{tot}} - 1$	$\mathrm{ref}_{\mathrm{tot}}$
$\nu = 1$	$\widetilde{\sigma}_h = \widetilde{\sigma}_h^{\mathrm{CEQ}}$	1.95	1.96	1.94	1.92	1.90
$\nu = 1$	$\sigma_h = \sigma_h^{\mathrm{GEQ}}$	1.00	1.00	1.00	1.00	1.00
$\nu = 1$	$\sigma_h = \sigma_h^{\mathrm{LEQ}}$	2.39	2.39	2.36	2.36	2.37
$\nu = 10^{-4}$	$\widetilde{\sigma}_h = \widetilde{\sigma}_h^{\mathrm{CEQ}}$	26.79	27.17	23.57	18.40	15.00
$\nu = 10^{-4}$	$\sigma_h = \sigma_h^{\mathrm{GEQ}}$	1.00	1.00	1.00	1.00	1.00
$\nu = 10^{-4}$	$\sigma_h = \sigma_h^{\mathrm{LEQ}}$	2.39	2.39	2.36	2.36	2.37

TABLE 3. Efficiency indices in the Example from Section 9.3 on the last five adaptively refined meshes using the SV element. Here $\mathrm{ref}_{\mathrm{tot}}$ denotes the total number of refinement steps.

pressure-robust one is even asymptotically exact, and all convergence rates are optimal. For $\nu = 10^{-4}$ the numbers and meshes for the pressure-robust estimator are exactly the same (which is expected, since the discrete velocity did not change), but the adaptive meshes for the classical estimator do not refine the corner singularity and therefore fail to reduce the velocity error optimally. Here, the refinement indicators only see the dominating pressure error and mark accordingly to reduce the pressure error. Adaptation to the corner singularity only starts when the velocity error and the pressure error scaled with ν^{-1} are on par. The slow decrease of the efficiency indices in Table 3 can be explained by the bestapproximation error reduction of the smooth pressure. Consequently,

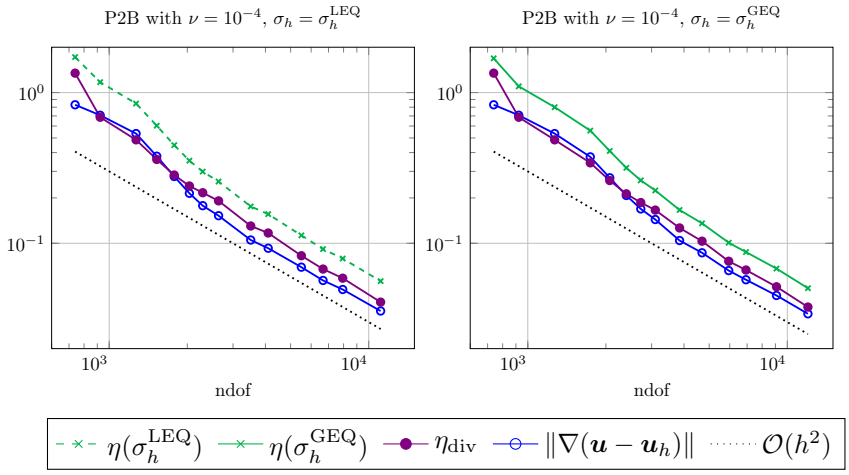

FIGURE 5. Example from Section 9.3: Convergence history of exact error and error estimators on adaptively refined meshes for P2B with $\nu = 10^{-4}$ and $\sigma_h = \sigma_h^{\mathsf{LEQ}}$ (left) and $\sigma_h = \sigma_h^{\mathsf{GEQ}}$ (right).

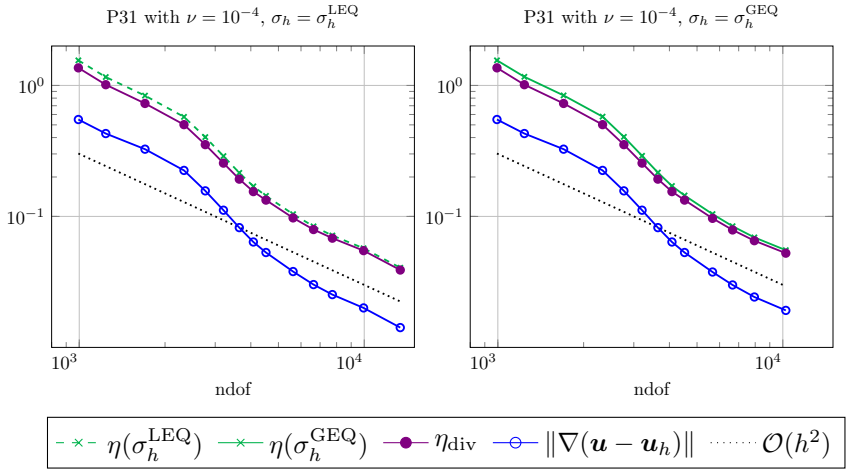

FIGURE 6. Example from Section 9.3: Convergence history of exact error and error estimators on adaptively refined meshes for P31 with $\nu = 10^{-4}$ and $\sigma_h = \sigma_h^{\mathsf{LEQ}}$ (left) and $\sigma_h = \sigma_h^{\mathsf{GEQ}}$ (right).

the exact velocity error on the final mesh obtained with refinement indicators based on $\widetilde{\sigma}_h^{\mathsf{CEQ}}$ is still larger by more than one order of magnitude compared to the error on the final mesh obtained with refinement indicators based on σ_h^{GEQ}. These observations also support the discussion in Remark 4.3.

Figures 5-7 display results for the three other methods P2B, P31 and P20 for the local and global variant of our pressure-robust error estimator. Since, the discrete velocity and the error estimator is independent of ν, we only show the results for $\nu = 10^{-4}$. Note that these methods are not divergence-free but pressure-robust due to their reconstruction operator in the right-hand side. However, this causes $\mathrm{div}(\boldsymbol{u}_h) \neq 0$ and hence the contribution η_{div} appears here which also requires a lower bound for the inf-sup constant c_0. Here, we take the value $c_0 = 0.3$ from [43]. Unfortunately, this has a significant impact on the efficiency of the error estimator that is largest for P20 and smallest for P2B leading to still very small efficiency indices between 1.5 and 3 for both the local and the global equilibration error estimators.

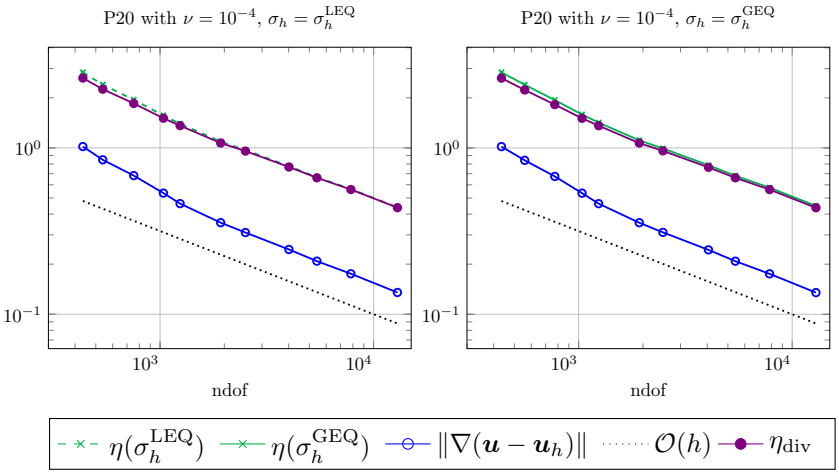

FIGURE 7. Example from Section 9.3: Convergence history of exact error and error estimators on adaptively refined meshes for P20 with $\nu = 10^{-4}$ and $\sigma_h = \sigma_h^{\mathrm{LEQ}}$ (left) and $\sigma_h = \sigma_h^{\mathrm{GEQ}}$ (right).

REFERENCES

[1] N. Ahmed, G. R. Barrenechea, E. Burman, J. Guzmán, A. Linke, and C. Merdon. A pressure-robust discretization of Oseen's equation using stabilization in the vorticity equation, 2020 (accepted by SINUM).

[2] M. Ainsworth and W. Dörfler. Reliable a posteriori error control for nonconformal finite element approximation of Stokes flow. *Math. Comp.*, 74(252):1599–1619 (electronic), 2005.

[3] F. Bertrand and D. Boffi. The Prager–Synge theorem in reconstruction based a posteriori error estimation, 2019.

[4] D. Boffi and L. Gastaldi, editors. *Mixed Finite Elements, Compatibility Conditions, and Applications*, volume 139 of *Lecture Notes in Mathematics*. Springer, April 2008.

[5] D. Braess and J. Schöberl. Equilibrated residual error estimator for edge elements. *Math. Comp.*, 77:651–672, 2008.

[6] P. Bringmann, C. Carstensen, and C. Merdon. Guaranteed velocity error control for the pseudostress approximation of the Stokes equations. *Numerical Methods for Partial Differential Equations*, 32, 04 2016.

[7] C. Carstensen, M. Eigel, R. H. W. Hoppe, and C. LÃűbhard. A review of unified a posteriori finite element error control. *Numerical Mathematics: Theory, Methods and Applications*, 5(4):509âĂŞ558, 2012.

[8] C. Carstensen and C. Merdon. Computational Survey on A Posteriori Error Estimators for the Crouzeix–Raviart Nonconforming Finite Element Method for the Stokes Problem. *Comput. Methods Appl. Math.*, 14(1):35–54, 2014.

[9] M. Costabel and A. McIntosh. On Bogovskiĭ and regularized Poincaré integral operators for de Rham complexes on Lipschitz domains. *Mathematische Zeitschrift*, 265(2):297–320, 2010.

[10] L. Demkowicz, P. Monk, L. Vardapetyan, and W. Rachowicz. De Rham diagram for hp finite element spaces. *Computers & Mathematics with Applications*, 39(7):29 – 38, 2000.

[11] P. Destuynder and B. Métivet. Explicit error bounds in a conforming finite element method. *Mathematics of Computation*, 68:1379–1396, 1999.

[12] A. Ern and M. Vohralík. Polynomial-degree-robust a posteriori estimates in a unified setting for conforming, nonconforming, discontinuous Galerkin, and mixed discretizations. *SIAM Journal on Numerical Analysis*, 53(2):1058–1081, 2015.

[13] R. Falk and M. Neilan. Stokes complexes and the construction of stable finite elements with pointwise mass conservation. *SIAM J. Numer. Anal.*, 51(2):1308–1326, 2013.

[14] N. R. Gauger, A. Linke, and P. W. Schroeder. On high-order pressure-robust space discretisations, their advantages for incompressible high reynolds number generalised beltrami flows and beyond. *The SMAI journal of computational mathematics*, 5:89–129, 2019.

[15] J. Gedicke, S. Geevers, I. Perugia, and J. Schöberl. A polynomial-degree-robust a posteriori error estimator for Nédélec discretizations of magnetostatic problems, 2020.

[16] Vivette Girault and Pierre-Arnaud Raviart. *Finite element methods for Navier-Stokes equations*, volume 5 of *Springer Series in Computational Mathematics*. Springer-Verlag, Berlin, 1986. Theory and algorithms.

[17] J. Gopalakrishnan, P.L. Lederer, and J. Schöberl. A mass conserving mixed stress formulation for Stokes flow with weakly imposed stress symmetry. *SIAM J. Numer. Anal.* To appear.

[18] J. Gopalakrishnan, P.L. Lederer, and J. Schöberl. A mass conserving mixed stress formulation for the Stokes equations. *IMA Journal of Numerical Analysis*, 05 2019.

[19] J. Guzmán and M. Neilan. Conforming and divergence-free Stokes elements on general triangular meshes. *Math. Comp.*, 83(285):15–36, 2014.

[20] A. Hannukainen, R. Stenberg, and M. Vohralík. A unified framework for a posteriori error estimation for the Stokes problem. *Numer. Math.*, 122(4):725–769, 2012.
[21] V. John, A. Linke, C. Merdon, M. Neilan, and L. Rebholz. On the divergence constraint in mixed finite element methods for incompressible flows. *SIAM Review*, 59(3):492–544, 2017.
[22] G. Kanschat and N. Sharma. Divergence-conforming discontinuous Galerkin methods and c^0 interior penalty methods. *SIAM Journal on Numerical Analysis*, 52(4):1822–1842, 2014.
[23] C. Kreuzer, R. Verfürth, and P. Zanotti. Quasi-optimal and pressure robust discretizations of the Stokes equations by moment- and divergence-preserving operators, 2020.
[24] P.L. Lederer. *A Mass Conserving Mixed Stress Formulation for Incompressible Flows*. PhD thesis, Technical University of Vienna, 2019.
[25] P.L. Lederer, C. Lehrenfeld, and J. Schöberl. Hybrid discontinuous Galerkin methods with relaxed h(div)-conformity for incompressible flows. part i. *SIAM Journal on Numerical Analysis*, 56(4):2070–2094, 2018.
[26] P.L. Lederer, A. Linke, C. Merdon, and J. Schöberl. Divergence-free reconstruction operators for pressure-robust Stokes discretizations with continuous pressure finite elements. *SIAM Journal on Numerical Analysis*, 55(3):1291–1314, 2017.
[27] P.L. Lederer, C. Merdon, and J. Schöberl. Refined a posteriori error estimation for classical and pressure-robust Stokes finite element methods. *Numerische Mathematik*, 142(3):713–748, Jul 2019.
[28] A. Linke. On the role of the Helmholtz decomposition in mixed methods for incompressible flows and a new variational crime. *Comput. Methods Appl. Mech. Engrg.*, 268:782–800, 2014.
[29] A. Linke, G. Matthies, and L. Tobiska. Robust arbitrary order mixed finite element methods for the incompressible Stokes equations with pressure independent velocity errors. *ESAIM: M2AN*, 50(1):289–309, 2016.
[30] A. Linke and C. Merdon. Guaranteed energy error estimators for a modified robust Crouzeix-Raviart Stokes element. *J. Sci. Comput.*, 64(2):541–558, 2015.
[31] A. Linke and C. Merdon. Pressure-robustness and discrete Helmholtz projectors in mixed finite element methods for the incompressible Navier-Stokes equations. *Comput. Methods Appl. Mech. Engrg.*, 311:304–326, 2016.
[32] A. Linke, C. Merdon, and M. Neilan. Pressure-robustness in quasi-optimal a priori estimates for the Stokes problem. pages 281–294. Online available: https://epub.oeaw.ac.at/?arp=0x003b8d45.
[33] R. Luce and B. Wohlmuth. A local a posteriori error estimator based on equilibrated fluxes. *SIAM J. Numer. Anal.*, 42:1394–1414, 2004.
[34] J. M. Melenk and C. Rojik. On commuting p-version projection-based interpolation on tetrahedra. *Mathematics of Computation*, 89(321):45–87, Jun 2019.
[35] C. Merdon. *Aspects of guaranteed error control in computations for partial differential equations*. PhD thesis, Humboldt-Universität zu Berlin, 2013.
[36] P. Monk. *Finite element methods for Maxwell's equations*. Numerical Mathematics and Scientific Computation. Oxford University Press, New York, 2003.
[37] P. Neittaanmäki and S. Repin. A posteriori error majorants for approximations of the evolutionary Stokes problem. *Journal of Numerical Mathematics*, 18(2):119 – 134, 2010.
[38] W. Prager and J. L. Synge. Approximations in elasticity based on the concept of function space. *Quart. Appl. Math.*, 5:241–269, 1947.
[39] S.I. Repin. *A Posteriori Estimates for Partial Differential Equations*. De Gruyter, Berlin, Boston, 2008.
[40] J. Schöberl. NETGEN An advancing front 2D/3D-mesh generator based on abstract rules. *Computing and Visualization in Science*, 1(1):41–52, 1997.
[41] J. Schöberl. C++11 Implementation of Finite Elements in NGSolve. *Institute for Analysis and Scientific Computing, Vienna University of Technology*, 2014.
[42] L. R. Scott and M. Vogelius. Conforming finite element methods for incompressible and nearly incompressible continua. In *Large-scale computations in fluid mechanics, Part 2 (La Jolla, Calif., 1983)*, volume 22 of *Lectures in Appl. Math.*, pages 221–244. Amer. Math. Soc., Providence, RI, 1985.
[43] G Stoyan. Towards discrete Velte decompositions and narrow bounds for inf-sup constants. *Computers & Mathematics with Applications*, 38(7):243–261, 1999.
[44] R. Verfürth. A posteriori error estimators for the Stokes equations. *Numer. Math.*, 55(3):309–325, 1989.
[45] J. Wang, Y. Wang, and X. Ye. Unified a posteriori error estimator for finite element methods for the Stokes equations. *Int. J. Numer. Anal. Model.*, 10(3):551–570, 2013.
[46] L. Zhao, E.J. Park, and E. Chung. A pressure robust staggered discontinuous Galerkin method for the Stokes equations, 2020.